University of Southern Queensland
Faculty of Engineering and Surveying

Porous Weirs for Flood Mitigation

A dissertation submitted by

Mr Joseph Ian Saunders

in fulfilment of the requirements of

Courses ENG4111 and 4112 Research Project

towards the degree of

Bachelor of Engineering (Civil)

Submitted: November 2007

ABSTRACT

Porous weirs offer an alternative design that could be adopted for flood mitigation.

The aim of this project is to construct and simulate a 1:25 scale model of a porous weir in the wide flume of the USQ hydraulics laboratory. The goal is to determine a relationship between upstream storage (depth) and the discharge of the weir to be use in being able to determine the flood mitigation potential of the porous weir.

The flow through the porous weir is to be analysed by analogy to the Darcy type equations and open channel flow equations. When the depth of flow exceeds the height of the weir an attempt will be made to fit a general weir type equation to the measured data.

Results have shown that turbulent flow exists in the model and that the traditional Darcy equation does not fit the flow through the weir. However a good relationship was found by analogy to the general equation of gradually varied flow when the flow was through the porous media. Once the flow exceeded the height of the weir it was found that the flow closely resembled the flow of a traditional hard weir.

LIMITATIONS OF USE

University of Southern Queensland

Faculty of Engineering and Surveying

ENG4111 Research Project Part 1 &
ENG4112 Research Project Part 2

Limitations of Use

Frank Bullen

Professor Frank Bullen
Dean
Faculty of Engineering and Surveying

CERTIFICATION

I certify that the ideas, designs and experimental work, results, analyses and conclusions set out in this dissertation are entirely my own effort, except where otherwise indicated and acknowledged.

I further certify that the work is original and has not been previously submitted for assessment in any other course or institution, except where specifically stated.

Joseph Ian Saunders
0050008157

__________________________ Signature

__________________________ Date

ACKNOWLEDGEMENTS

This research was carried out under the principal supervision of Ken Moore, a lecturer at the University of Southern Queensland.

I would also like to thank the lab staff for the construction of the wire aggregate cage.

TABLE OF CONTENTS

Contents | Page

LIST OF FIGURES

Figure Page

LIST OF TABLES

Table | Page

NOMENCLATURE

A	= the macroscopic cross sectional area, m^2
C_g	= coefficient of graduation
C_u	= coefficient of uniformity
d	= characteristic length, m
d_d	= depth of the flow exiting the face of the weir, m
d_{df}	= depth of the flow downstream of the weir, m
d_m	= mean particle diameter, m
d_o	= depth of the flow over the downstream face of the weir, m
d_u	= depth of the flow upstream of the weir, m
d_x	= particle size greater than X% by weight, m
f	= friction factor
F_G	= geometric scaling factor
F_K	= kinematic scaling factor
g	= acceleration due to gravity, 9.81 m/s^2
h_f	= head loss due to friction, m
h_L	= head loss, m
H	= head, m
H_d	= head at the downstream face of the weir, m
H_{df}	= head of the flow downstream of the weir, m
H_u	= head of the flow upstream of the weir, m
i	= hydraulic gradient, m/m
k	= coefficient of permeability, m/s
K	=intrinsic permeability, m^2
L	= length of flow path, m
L_T	= length over the top of the weir, m
n	= porosity
Q	= total discharge, m^3/s
Q_{Ideal}	= ideal discharge, m^3/s
R	= hydraulic radius, m
Re	= Reynolds number

V = actual velocity, m/s

V_B = macroscopic velocity, m/s

V_b = bulk volume, m^3

V_s = volume of solids, m^3

V_v = volume of voids, m^3

y = depth of flow, m

w = width of the channel, m

γ =specific weight of fluid (N/m^3)

$\Delta\varphi$ = head drop in the direction of flow, and;

ρ = density, 1000 kg/m^3

ν = kinematic viscosity, m^2/s

μ = dynamic viscosity, 0.001 Ns/m^2

CHAPTER 1- INTRODUCTION

1.1 Purpose of study

One of the implications of urban development is that there is a corresponding increase in the generation of stormwater runoff. The reason for this increase in runoff is the increase in the sealed or impervious area such as roads, driveways and roofs. These areas allow far less infiltration than the original bare or grassed surface and therefore a greater quantity of rainfall then becomes runoff. Another factor that contributes significantly to increased runoff is the reduced time of concentration of a catchment due to increased channelisation (kerb and channel, and stormwater pipes) that accompanies the development. Essentially the development removes some of the naturally occurring detention of stormwater.

Porous weirs could be used in conjunction with a detention basin in such projects as urban developments where it is desirable to maintain the predevelopment runoff hydrograph. This may be due to the capacity of the downstream stormwater system being at capacity under a particular storm event; therefore there can be no net increase in the runoff (particularly the peak flow) from the catchment. This situation has been adopted by some local councils where it is specified in the development conditions that there be a non-worsening effect created by the proposed development.

The purpose of this study is to evaluate the performance of a porous weir by analysis different stages of flow and to develop head discharge relationship for the porous weir.

1.2 Research objectives

The objectives of this project are formally outlined in the project specification in Appendix A.

The first objective of this project is to conduct a literature review to determine design parameters and standards, and hydraulic performance of various flood mitigation structures for urban stormwater drainage with particular emphasis on weirs. This is to include any published data concerning the head discharge characteristics of porous weirs.

Following the research, design of a model weir will be undertaken and will incorporate important parameters found in the literature review. Construction of the weir will then take place using appropriate materials.

The weir will then be modelled in the USQ hydraulics laboratory. Measurements will be taken for a range of head and tail water conditions to determine the performance of the weir. These measurements will then be analysed with respect to the physical characteristics of the weir to determine a relationship between the head and the discharge using known parameters of the porous media.

The research is expected to result in the determination of the characteristics that effect the flow through a porous weir and will allow them to be used effectively in the design and modelling of catchments.

A review of the literature for this research will identify the design parameters that will influence the performance of the weir. It will also give an indication of what porous structures are currently used and the components that control the performance of the structure.

The outcomes of this study could be used in the design of control structures for waterways to reduce flooding.

CHAPTER 2- LITERATURE REVIEW

2.1 Introduction

A literature review was undertaken to establish what parameters would need to be considered to determine the hydraulic performance of the porous weir.

The literature review was also used to establish whether any studies have previously been undertaken to determine the performance of a porous weir structure. Any design data that could be collected would be useful in the analysis of the porous weir.

2.2 Background study

2.2.1 Properties of the fluid

The fluid to be used in the testing of the porous weir is to be water. The properties of the fluid that are of particular interest are the density and the viscosity.

The density (ρ) is the mass per unit volume and at 20°C is equal to 1000kg/m^3. Although this value varies with temperature and pressure, any reference to density in this paper will refer to that of 1000kg/m^3 unless specified otherwise.

The other key fluid property is viscosity. Viscosity is 'a measure of the reluctance of the fluid to yield to shear when the fluid is in motion' (Bear, p. 32) and can be quantified in two different ways, kinematic viscosity (ν) and dynamic viscosity (μ). The relationship between kinematic viscosity and dynamic viscosity is as follows,

$$\nu = \frac{\mu}{\rho}.$$

…Equation 2.1

Although the value of viscosity varies with temperature, any reference to the dynamic viscosity 0.001Ns/m^2, value at 20°C, unless specified otherwise.

2.2.2 Properties of the porous media

The properties of the porous media that are of particular interest are the porosity, particle size distribution and the packing arrangement.

The porous media can be described by the characteristic length of the individual particles. This can be determined by measuring the particle size distribution via a sieve analysis. The grading of the particles is determined by plotting the percentage passing by weight against the particle diameter on a log-normal graph. This then allows the particle size distribution to be categorised into three different categories; well graded (many different particle ranges), uniform graded (single range of particles) or gap graded (one or more particle ranges missing).

The diameter of the particle size that is greater than *X%* of the particles by weight is known as d_X. It can be seen in section 2.2.3 that the value of d_{50} will be of importance in determining Reynolds Number.

Some dimensionless coefficients used to describe the particle size distribution that could be important are Hazen's effective Coefficient of Uniformity (C_u),

$$C_u = \frac{d_{60}}{d_{10}} ,$$

…Equation 2.2

and the Coefficient of Gradation (C_g),

$$C_g = \frac{(d_{30})^2}{d_{60} \times d_{10}}.$$

…Equation 2.3

Porosity is another important parameter of the media. The porosity (n) is the ratio of void space to the bulk volume and is usually expressed as a percentage.

$$n = \frac{V_v}{V_b} = \frac{V_b - V_s}{V_b},$$

…Equation 2.4

where;

V_v = volume of the voids,
V_b = bulk volume, and;
V_s = volume of the solids

Porosity is a function of the shape of the particle and packing arrangement. If the diameter of the particle is increased and the shape and packing arrangement remain constant, then the porosity will remain the same. Bear (1988, p. 46) reports the range of porosities that exist for some common materials. Some materials that are of interest to this study are gravels for which the range of porosities range from 30-40% and gravel and sand mixes for which the porosity ranges from 30-35%.

Bear (1988, p. 47) also gives some approximate values of porosity for different possible gradings of gravel. These values show that a well-sorted distribution has a porosity of approximately 32%.

The porosity is an important parameter of the porous media as it gives an indication of the size of the flow paths through the porous media. The porosity of the porous media can be determined by measuring the amount of water required to fill the void of the porous media. The ranges of porosity presented by Bear (1988) can be used to verify the measurements taken during the testing of the porous media.

2.2.3 Darcy's equation

Many porous flow analysis' reports begin with Darcy's equation for flow of water through porous media, which was developed by Darcy in 1856 by investigating flow through vertical homogeneous sand filters (Bear 1988, p. 119). Darcy's investigation showed that

$$Q \propto A,$$

And developed the equation;

$$Q = k \times i \times A, \qquad \text{…Equation 2.5}$$

where;

Q = total discharge (m^3/s),
k = coefficient of permeability (m/s),
i = hydraulic gradient (m/m), and;
A = cross sectional area (m^2).

The coefficient of permeability, *k*, (also known as coefficient of proportionality or as hydraulic conductivity) is a value that represents the resistance of the porous media to the flow (Das, 1985) and is dependant upon both the properties of the media and the fluid (Bear 1988 p. 132). This value has the units of length per unit time and is commonly encountered in Darcy's equation. Permeability can also be represented by the intrinsic permeability, *K*, which is measured with the units of length squared. The intrinsic permeability is a function of the properties of the porous media and is independent of the fluid flowing through it. The intrinsic permeability is related to the coefficient of permeability by the following equation.

$$k = \frac{K \times \rho \times g}{\mu},$$

…Equation 2.6

where;

k = coefficient of permeability (m/s),
K = intrinsic permeability (m^2),
ρ = mass density of fluid (kg/m^3),
g = acceleration due to gravity (m/s^2), and;
μ = dynamic (or absolute) viscosity ($N.s/m^2$).

Michioku et al. (2005) reports that Shimizu et al. used a linear relationship between mean particle diameter and coefficient of permeability where,

$$\sqrt{K} = e \times d_m$$
$$K = (e \times d_m)^2,$$

…Equation 2.7

where;

e = 0.028 (a constant determined by Michioku et al.), and;
d_m = mean particle diameter of media (m).

The intrinsic permeability will be calculated as a constant if the above equation is used and, if applied to equation 2.6 will yield a constant value for the coefficient of permeability. This is in line with the coefficients of permeability reported in engineering textbooks as being a constant value for a given type of porous media. Studies done by Michioku, et al. (2005) have shown that the value of *e* shown above may only be valid for confined porous media flows (impermeable surface in all directions perpendicular to the direction of flow). Their studies have shown that, for unconfined porous media flow (subject to atmospheric pressure at the free surface) associated with open channels, a value of e equal to 0.0196 is more appropriate.

Darcy's equation incorporates a value known as the hydraulic gradient. The hydraulic gradient is the head loss per unit length of flow caused by the interaction between the fluid and porous media and is represented by the equation,

$$i = \frac{h_L}{L},$$

…Equation 2.8

where;

h_L = head loss (m), and;
L = length of flow (m).

2.2.4 Non-Darcian flow

Studies by many including Venkataraman and Rama Mohan Rao (1998) have shown Darcy's law to only be accurate when the flow through porous media is laminar.

Laminar flow in pipes is defined by Reynolds Number. Reynolds Number is the ratio of the effects of inertia to viscosity. If Reynolds number is low then the viscous forces control the flow and the flow is laminar. The upper limit of laminar flow in pipes is represented by Reynolds numbers equal to 2100 (Bear 1988, p. 125). By analogy Reynolds number can be used to represent laminar flow in porous media. Reynolds number (Re) is calculated by the following equation, which is generally associated with pipe flow;

$$\mathrm{Re} = \frac{\rho \times V \times d}{\mu} = \frac{V \times d}{\nu},$$

…Equation 2.9

where;

V = velocity (m/s), and;
d = diameter of the pipe (m).

In previous studies investigating flow through porous media an adaptation of the above equation has been used to calculate a representative value for Reynolds number. This has been done by using a characteristic length of the porous media to define the pipe diameter.

In various studies the characteristic length is defined differently and Bear (1988) and Kirkham (1967) report that as Reynolds number is analogous to pipe flow then '*d*' should also be analogous to pipe flow and represent a dimension of the flow path. Some of the definitions of '*d*' are reported below.

Bear (1988) references that Collins (1961) suggested,

$$d = \left(\frac{k}{n}\right)^{1/2}.$$

…Equation 2.10

Bear also reports that Ward (1964) used,

$$d = (k)^{1/2},$$

…Equation 2.11

and also uses,

$$d = d_{50},$$

to define the characteristic length in the calculation of Reynolds Number.

The upper limit of the laminar zone is reported to be Reynolds number equal to 10 in porous media flow (Bear, 1988), as long as the characteristic length used to calculate Reynolds Number is the average grain diameter (d_{50}). Although this value does not directly represent a dimension of the flow path it is suggested that it has been widely used due to the relative ease of measuring the quantity. Because the average grain diameter has been widely used the Reynolds number in this paper will be calculated using the following equation to establish whether laminar flow exists.

$$\mathrm{Re} = \frac{V \times d_{50}}{\nu},$$

…Equation 2.12

where;

V = macroscopic velocity (m/s).

The macroscopic velocity is used in the calculation of the Reynolds number, as it is difficult to determine the actual velocity of the flow. The macroscopic velocity is equal to the discharge divided by the bulk cross sectional area of the flow.

Studies have been undertaken to define the complete range of flows through porous media especially where the flow is no longer laminar. Such studies as those by and reported Venkataraman and Rama Mohan Rao (1998) and Bear (1988) have shown that the flow has a transitional zone in between the laminar and turbulent zones. Proposed variations to Darcy's equations to describe these transitional and turbulent flows are;

$$V = k \times i,$$

…Equation 2.13

where;

V = discharge velocity (m/s), and;

i = hydraulic gradient defined as a function of velocity as follows.

The equations shown below have been reported by Venkataraman and Rama Mohan Rao (1998) and have been used to define the hydraulic gradient once the flow is no longer laminar, (Missbach);

$$i = C \times V^{m},$$

…Equation 2.14

where;

C = a coefficient determined experimentally, and;

m = an index determined experimentally.

(Forchheimer);

$$i = aV + bV^{2},$$

…Equation 2.15

where;

a = a constant representing fluid properties, and;

b = a constant representing media properties.

Kirkham (1967) also reports (Forchheimer);

$$i = aV + bV^{2} + cV^{n},$$

…Equation 2.16

where;

c = a parameter.

and (Chalmers, Taliaferro and Rawlins);

$$i = aV + bV^n$$

…Equation 2.17

where;

n = index ranging from 1.753 - 2.018.

Venkataraman and Rama Mohan Rao (1998) reported that Ward (1964) created equations for '*a*' and '*b*' based on Forchheimer's equation;

$$i = aV + bV^2,$$

where;

$$a = \frac{\mu}{\rho \times g \times K} \text{ and;}$$

…Equation 2.18

$$b = \frac{C_w}{g\sqrt{K}},$$

…Equation 2.19

where;

C_w = a media constant determined experimentally.

Venkataraman and Rama Mohan Rao (1998) also reported that Ahmed and Sunada (1969) created equations for '*a*' and '*b*';

$$a = \frac{\mu}{\rho \times g \times K} \text{ and;}$$

…Equation 2.20

$$b = \frac{1}{g\sqrt{c \times K}}$$

…Equation 2.21

where;

$K = c \times d^2$, where 'd' is determined after experimentally determining 'a' and 'b'

The two equations for *b* are related by the formula,

$$C_w = \frac{1}{\sqrt{c}} = \frac{d}{\sqrt{K}}.$$

…Equation 2.22

where;

$$c = \frac{a}{b^2 \times g \times v},$$

where c is determined after experimentally determining b.

Ward (Venkataraman and Rama Mohan Rao, 1998) obtained an expression for friction factor based on a Reynolds number and C_w,

$$f_K = \frac{1}{R_K} + C_w,$$

…Equation 2.23

where;

$$R_K = \frac{V \times \sqrt{K}}{\nu}.$$

…Equation 2.24

Venkataraman and Rama Mohan Rao (1998) presented equation 2.24 in a graphical form based on data that had been collected from published work. The result is shown in the figure 2.1.

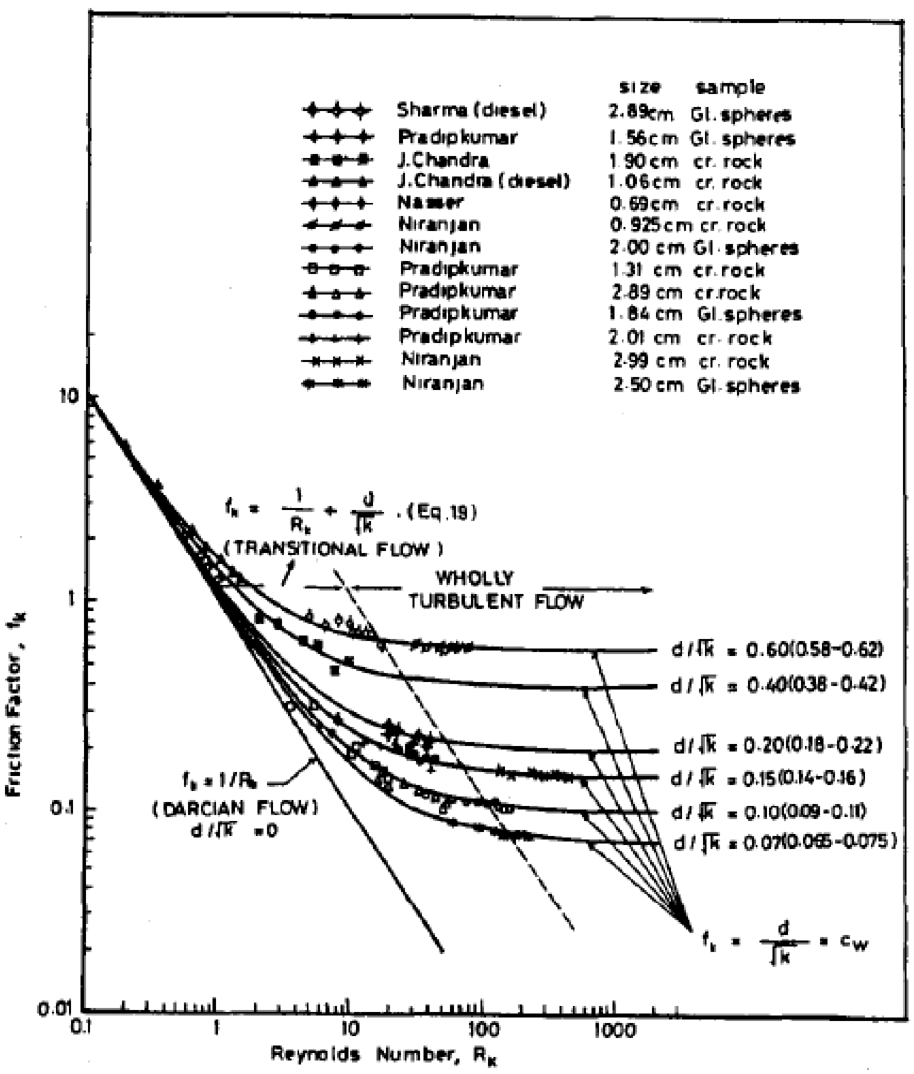

Figure 2.1 Reynolds number versus Friction Factor as shown by Venkataraman and Rama Mohan Rao (1998)

The Reynolds numbers shown in the figure 2.1 can be used to verify laminar or turbulent flow as the types of flow in the figure are clearly defined.

2.2.5 Analogy to Darcy-Weisbach equation

An equation to define the friction factor can be established by developing porous media flow equations analogically to flow through pipes and adopting the Darcy Weisbach equation. The Darcy-Weisbach equation is,

$$h_f = \frac{f \times L \times V^2}{2 \times g \times d},$$

…Equation 2.25

where;

h_f = head loss due to friction (m),
f = friction factor,
L = length of pipe (m),
V = velocity (m/s), and;
d = pipe diameter (m).

In this equation the hydraulic radius of the pipe is defined as,

$$R = \frac{d}{4},$$

…Equation 2.26

for pipes flowing full, the friction factor is equal to,

$$f = 2 \times d \times \frac{h_f}{L} \times \frac{g}{V^2}$$

…Equation 2.27

In Bear (1988, page 126) presents a Darcy-Weisbach equation analogous to porous media flow. The equation is given as;

$$\frac{\Delta\varphi}{L} = \frac{f \times V^2}{2 \times g \times d},$$

…Equation 2.28

where;

$\Delta\varphi$ = the head drop in the direction of flow, and;

L = length of the flow path.

Bear also presents the following friction factor proposed by Fanning called Fanning friction factor.

$$f_f = \frac{d}{2} \times \frac{\Delta\varphi}{L} \times \frac{\gamma}{\rho \times V^2},$$

…Equation 2.29

where;

f_f = Fanning friction factor,

γ = specific weight of fluid (N/m^3), and;

d = characteristic length of the media.

Fanning friction factor has been presented in a Moody type diagram of Reynolds number versus Fanning friction factor. Here the characteristic length used in the calculation of Fanning friction factor and Reynolds number is the same characteristic length.

$$\mathrm{Re} = \frac{V \times d_{50}}{\nu},$$

…Equation 2.30

Figure 2.2 clearly shows a straight section of the plot, which represents laminar flow where the Fanning friction factor is reported to equal,

$$f_f = \frac{1000}{\mathrm{Re}}.$$

…Equation 2.31

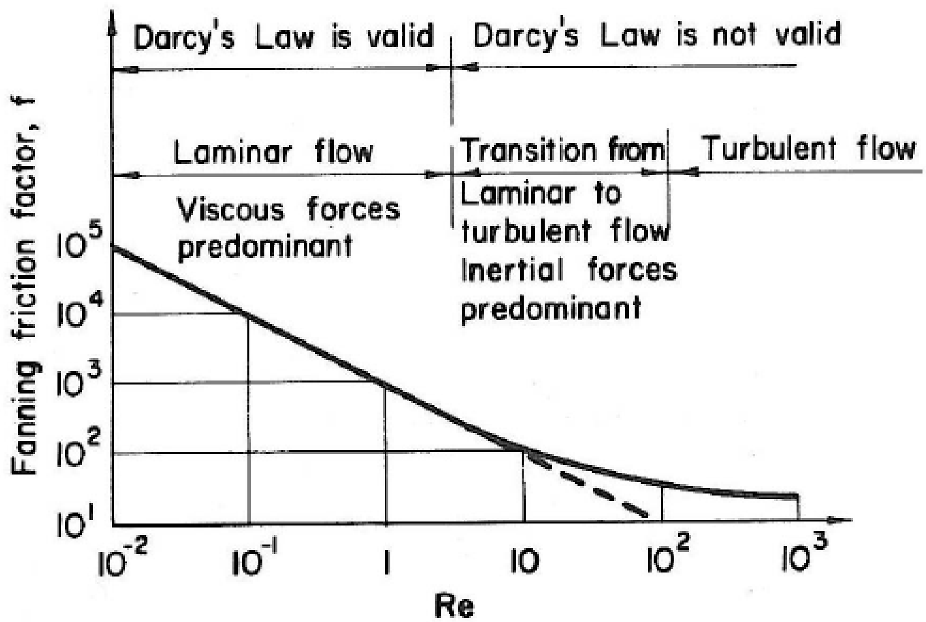

Figure 2.2 Reynolds number versus Fanning Friction Factor as presented by Bear (1988)

Since the flow through the porous weir will have a free surface, similar to open channel flow, some open channel flow equations may be investigated to determine if a relationship exists. The following are some formulae relating to flows with a free surface.

Manning's equation,

$$Q = \frac{A \times R^{2/3} \times \sqrt{S_0}}{n},$$

…Equation 2.31

where;

S_0 = slope of the channel bed, and;
n = Manning's roughness coefficient

When overflow of the weir is achieved it is expected that the performance of the weir will resemble that of the performance of a broad crested hard weir. The formula commonly used to represent the ideal flow over a broad crested hard weir is,

$$Q = C \times H^{3/2},$$

…Equation 2.32

where;

Q = discharge (m^3/s),
C = coefficient of discharge, and;
H = head based on the height above the top of the weir (m).

Chadwick and Morfett (2002) also present an equation for the ideal flow over a broad crested hard weir that does not account for any losses. The equation is,

$$Q_{Ideal} = \sqrt{g} \times w \times \left(\frac{2}{3} \times H\right)^{3/2},$$

…Equation 2.33

where;

w = width of the top of the weir (m).

In open channel flow the head (energy) at any given point can be calculated based on the equation,

$$H = y + \frac{\alpha \times V^2}{2 \times g},$$

…Equation 2.34

where;

y = the depth of the flow, and;
α = energy coefficient.

In this paper α will be assumed to be equal to a value of unity.

2.3 Design Standards for porous weirs

No specific design standards were found on the design of porous weirs although guidelines were found on the design of certain porous structures in the Main Roads, Road drainage design manual (2002). These porous structures include check dams, rock sediment traps and sediment basins.

The check dams discussed in the Road drainage design manual are used to slow the discharge velocities in a channel. These dams are generally created from medium sized rock or sand/gravel filled bags. The rock size adopted is generally 200mm.

Rock sediment traps are generally used as temporary structures on construction sites. The rock to be used in this type of structure is described as well graded, hard and erosion resistant. The minimum sizing of the aggregate is recommended to be d_{50} of 225mm and a maximum of 350mm. Another interesting design feature is that the foundations are covered with a filter fabric to prevent ‘piping’. Downstream scour protection is also required to prevent erosion of the outlet. Other specifications include a minimum top width of 1.5m, maximum upstream face slope of 1(V):2(H) and a maximum downstream face of 1(V):3(H) to maintain stability of the structure. These values will be used as a guide to the sizes and gradings used in the porous weir model.

In AS2758.4-2000, Aggregate for gabion baskets and wire mattresses, specifications are set out for the size and durability requirements of the aggregate in gabion baskets. As the structure being modelled is similar to that of a gabion these specifications could be adopted for the design of the porous weir.

2.4 Design Parameters for porous weirs

In the design of the weir it is necessary to consider the top width of the weir and the up and downstream batters. These components influence the stability of the weir.

The particle size and grading of the rocks used in the weir are of particular importance, as it will determine the porosity of the weir. It is expected the flow rate through the weir and the headwater will be affected by this component of the design.

2.5 Hydraulic Performance

Michioku et al. have identified three different phases of flow associated with the porous weir. They are submerged, transient and overflow and are shown below in figure 2.3. It is expected that the weir will be used as a flood mitigation structure and therefore all three phases will be encountered within its lifecycle. Therefore an attempt will be made to model all three phases. The three different phases are expected to vary the relationship between storage and discharge and also affect the stability of the weir as a structure.

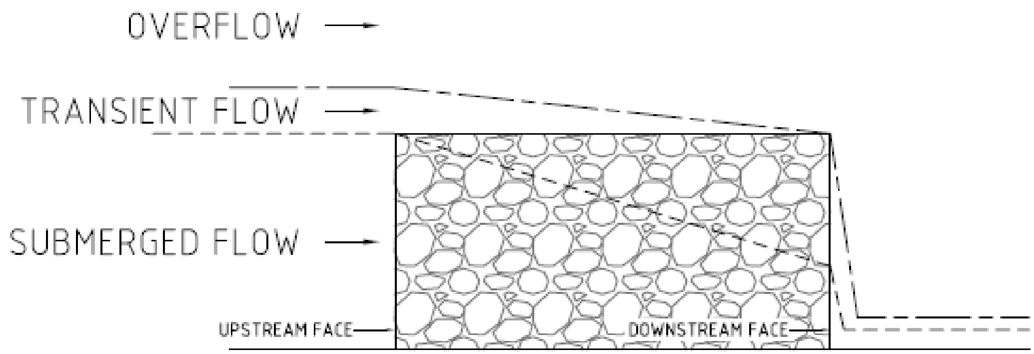

Figure 2.3 Submerged, transient and overflow

Figure 2.3 shows the limits of the three phases of flow.

The submerged phase is where the entire flow enters the weir through the vertical upstream face of the weir and exits through the vertical downstream face of the weir. It is expected that this phase will be completely dependent on the properties of the porous media.

The transient phase is identified when the free surface enters the weir through the top horizontal surface of the weir. Here there is a measurable depth over the upstream face of the weir. The entire discharge still exits the weir through the downstream vertical face of the weir.

The third phase is overflow. Overflow is defined when the weir is completely overtopped with the flow. There is a measurable depth of discharge at both the upstream and the downstream vertical faces of the weir.

2.6 Scale Modelling

Geometric, kinematic and dynamic similitude will need to be achieved for the model to accurately represent the performance of the weir prototype.

As the flow has a free surface, it is expected that Froude scaling will be used in the design of a scale model for testing.

In the prototype, it is not expected that the velocity will be slow enough for the effects of viscosity to govern losses, therefore flow should not be laminar and it is not expected that Reynolds scaling will be required.

If the flow is turbulent Darcy's equation will not be valid as it is only applicable to laminar flow. However there have been variations of Darcy's equation presented in the literature review that will be investigated in order to determine a relationship for the porous weir flow.

Other equations presented in the literature review relating to the turbulent open channel flow will also be applied to the measured data to determine if a correlation exists with the measured data.

CHAPTER 3- WEIR DESIGN

3.1 Introduction

This chapter aims to present the process and procedures undertaken in the design of the weir. It also aims to outline the considerations and assumptions made in the design process. Construction drawings are in Appendix B.

3.2 Design considerations

The first considerations made in the design of the weir were the dimensions and performance characteristics of the wide flume in the USQ hydraulics laboratory. The depth and width dimensions of the flume are 125mm x 610mm. The critical dimension here is expected to be the depth as the weir is to be designed to take flow through the porous media and have sufficient clearance to allow overflow of the structure. These dimensions will also be used in the consideration of the scaling ratio required between the model and prototype as this ratio is dependent upon the height of the weir and the depth of the flume.

Also considered at this stage was the aggregate size to be used in the model. Again this would need to be scaled up to represent the aggregate size in the prototype. The scale ratio is dependant upon the minimum and maximum particle sizes to be adopted in the actual sized model. This parameter is also critical as it could determine whether the flow is laminar or turbulent through the weir and will result in determining the type of scaling used. This parameter will also be influential in the upstream depth required to create overflow of the weir.

In the design of the cage it was required to produce a structure that was strong enough to withstand the forces of the water and the aggregate within the cage, and to have minimal impact on the flow of water through the media being contained. A wire cage of a small gauge (3mm) was adopted. Design drawings of the aggregate cage can be seen in Appendix B. The frame was strengthened the addition of bracing in the direction of flow. It is expected that a small aggregate will easily surround the bracing frames and prevent channelised flow from forming in these sections.

A 2mm thick rubber base was chosen to hold the aggregate from the underside of the weir. This would be strong enough to allow the weir to be handled when filled with aggregate and would also prevent the weir from sliding in the flume.

To prevent the aggregate from being washed away the cage needed a porous encasing membrane to retain the aggregate that would not control the flow of the water through the weir. An aluminium flyscreen was chosen as an appropriate material to hold the aggregate in the cage whilst it was being modelled. The aluminium flyscreen was laced to the framing using 0.25mm diameter fishing line. An aluminium flyscreen was chosen as it was of a smaller gauge and had larger holes than the nylon variety and therefore would cause less resistance to flow. As such, a better relationship would be obtained between the flow and the aggregate in the cage. During the experimental stage the cage will be tested to show that the aggregate in the cage controls the flow and not the aluminium flyscreen.

Lids were also constructed and flyscreen laced to these frames. These were used to prevent the aggregate from being washed out during the modelling of the weir.

Figure 3.1 shows the design features of the weir once it was constructed.

Figure 3.1 Constructed weir minus the porous media

3.3 The Model

From the background study, the most commonly adopted design for weirs is with the upstream and downstream faces battered. This design was avoided in the model as it was assumed that it would be easier to model a weir with a rectangular cross section. Rectangular structures have also been commonly adopted in the literature reviewed.

As the depth of the flume is only 125mm the maximum height of the weir was adopted as 80mm. It was assumed that this would allow sufficient upstream depth (40mm) to allow a range of different flows including overflow of the weir. The weir needs to be of sufficient height to take a series of measurements, with significant variation in the depth and flow rate, in each of the phases to allow an accurate representation of the flow to be established. For a weir depth of 80mm it is anticipated that a good range of measurements will be able to be achieved.

A 2m deep detention basin is a commonly adopted depth for an urban detention basin (Mainwaring, A 2007 pers. comm., 28 October). This generally allows for sufficient storage upstream of the basin outlet, to attenuate the runoff hydrograph on a small development catchment, whilst taking up only a small amount of surface area and maintaining public safety.

By adopting a maximum model height of 80mm the scaling factor for geometric scaling would be,

$$F_G = \frac{L_p}{L_m} = \frac{2}{0.08} = 25\,,$$

…Equation 3.1

where;

F_G = geometric factor,

L_p = a geometric dimension of the prototype (m), and;

L_m = corresponding geometric dimension of the model (m).

The maximum particle size was then calculated and found to be 10mm,

$$d_m = \frac{d_p}{F_G} = \frac{250}{25}\,,$$

where;

d_p = a particle size in the prototype (m), and;

d_m = corresponding particle size in the model (m).

As turbulent flow is expected, Froudes scaling is to be used to the related the velocity of the model to the velocity of the prototype.

$$F_K = \frac{V_m}{V_p},$$

…Equation 3.2

$$Fr = \frac{V}{\sqrt{g \times y}},$$

$$Fr_m = Fr_p,$$

$$\frac{V_m}{\sqrt{g \times y_m}} = \frac{V_p}{\sqrt{g \times y_p}},$$

$$F_K = \frac{V_m}{V_p} = \frac{\sqrt{g \times y_m}}{\sqrt{g \times y_p}},$$

$$F_K = \frac{\sqrt{y_m}}{\sqrt{25 y_m}} = \frac{1}{5},$$

…Equation 3.3

where;

F_K = kinematic factor,

V_p = a velocity in the prototype (m/s),

V_m = corresponding velocity in the model (m/s),

Fr = Froudes Number,

y_p = a depth in the prototype (m),

y_m = corresponding depth in the model (m).

A crushed rock aggregate was obtained from the USQ, for use as the porous media, for use in the porous weir. The d_{50} particle size adopted for the aggregate is equal to 5.725mm. Calculation of this value is discussed in chapter 4.

When calculating Reynolds number using the equation reported by Bear (1988), if Reynolds number is greater than 10, the flow in the model will be transitional or turbulent so long as the characteristic length used is the mean particle diameter and the velocity is the macroscopic velocity.

$$\mathrm{Re} = \frac{V_m \times d_{50}}{\nu},$$

$$V_m = \frac{\mathrm{Re} \times \nu}{d_{50}} = \frac{10 \times 1 \times 10^{-6}}{0.0057} = 0.00175 m/s.$$

If Reynolds number is above 100 the flow is expected to be turbulent (Bear 1988, p. 127),

$$\mathrm{Re} = \frac{V_m \times d_{50}}{\nu},$$

$$V_m = \frac{\mathrm{Re} \times \nu}{d_{50}} = \frac{100 \times 1 \times 10^{-6}}{0.0057} = 0.0175 m/s.$$

CHAPTER 4- EXPERIMENTAL METHODOLOGY

4.1 Introduction

The experiment was run in the wide flume of the USQ hydraulics laboratory.

This chapter is to report on the experimental procedure and the measurements taken. The chapter will then go on to discuss and analyse the measurements taken and assumptions and conclusions made from them.

4.2 The Procedure

As the aggregate used in the experiment will play an important role in the performance of the weir it is important to know several characteristics of the aggregate.

An aggregate was obtained from the USQ for the project. Measurements were taken on this aggregate before its use in the model. The first measurements were achieved by passing the aggregate through a series of sieves. This was done to ensure an accurate measurement of particle size was achieved. The aggregate was passed through a 6.7mm sieve and retained on a 4.75mm sieve to ensure that the particles were all within this range. Finer measurements of the aggregate were not taken as these two sieves were the two closest for this size range. As there is a small range of particle sizes that may have been included in the aggregate, d_{50} in the model and in the analysis of the experimental measurements will be taken as 5.725mm, which is the mid value of the two sieves employed.

As the aggregate size is smaller (5.725mm) than anticipated, the prototype aggregate size becomes 143mm due to the scale ratio being 1:25.

Based on the size of the aggregate used in the model, the media is defined as fine gravel.

Because the gravel adopted is of a single grade C_u and C_g cannot be calculated.

Measurements of the porosity of the aggregate were also taken. This was done by filling a container to a known volume (V_b) with aggregate and filling the void (V_v) with water. The porosity was then calculated using equation 2.4, and is as shown in table 4.1.

Table 4.1 Measurements and calculation of porosity

Bulk Volume, V_b (mL)	Void Volume, V_v (mL)	Porosity, n (%)
260	100	38.46
465	185	39.78
475	165	34.74
	Average	37.66

To gauge the performance of the porous weir measurements of depth and discharge were taken. The flow rates were obtained from the modelling of the weir via an electronic flow meter and in the units of litres per minute. The output from the flow meter was accurate to the nearest litre and therefore the readings taken may be in error to the magnitude of ±0.5L. The measurements of depth were taken with a suspended depth gauge as shown in figure 4.1. The readings are taken from a ruler mounted over the flume. The graduations on the ruler are in millimetres; therefore the accuracy of the measurements taken is ±0.5mm.

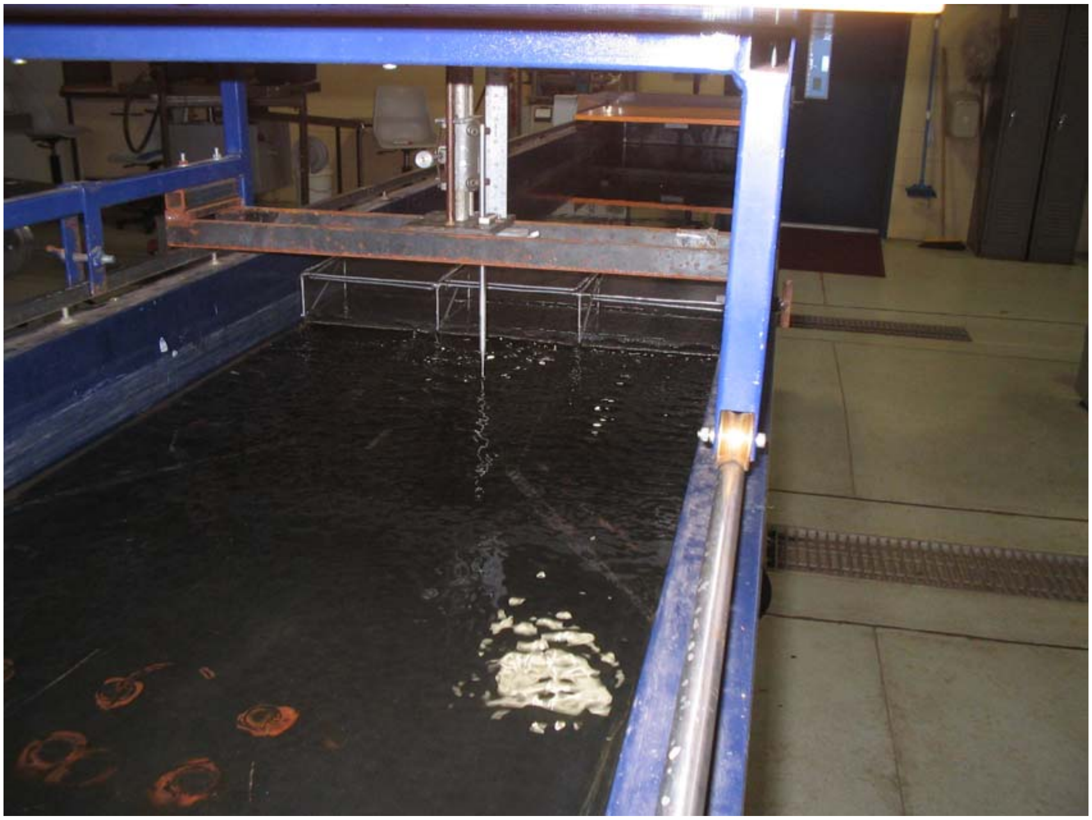

Figure 4.1 Suspended depth gauge

Before the aggregate cage was filled with the gravel, the empty weir was placed in the wide flume as can be seen in figure 4.2 and was subjected to a range of flows. This was done to establish the magnitude of losses that would be imposed by the flyscreen mesh that was adopted to hold the aggregate. The depth of the water was measured approximately 200mm upstream of the weir and central to the flume. The measurements taken are shown in table 4.2.

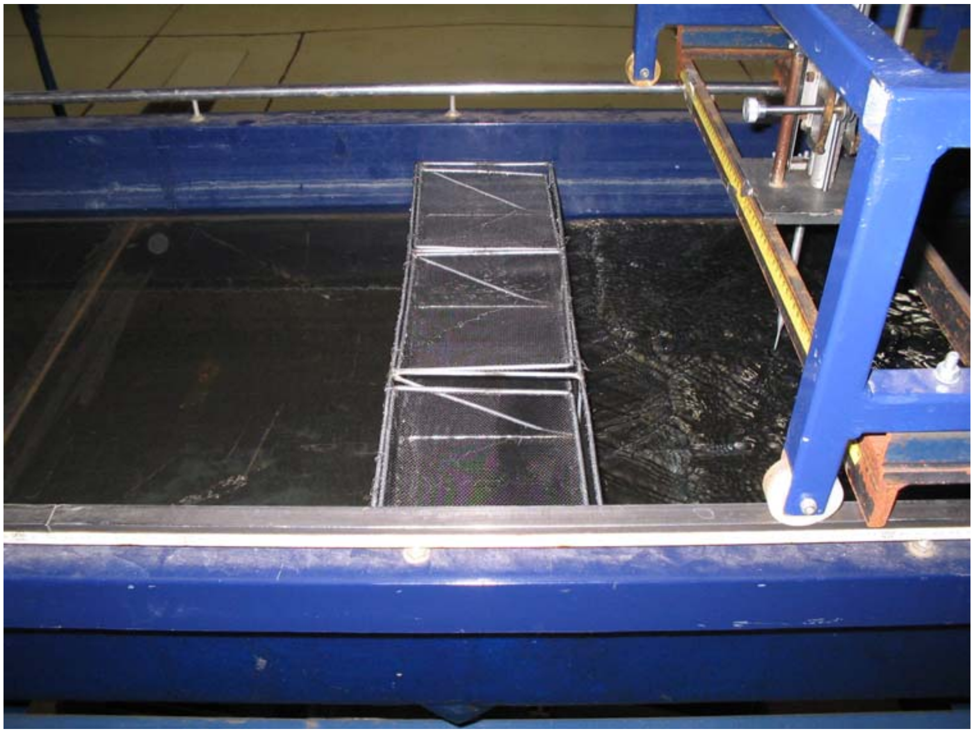

Figure 4.2 Testing the empty aggregate cage in the wide flume

Table 4.2 Measurements of flow through the empty cage

Q (m^3/s)	Depth upstream of the weir (m)	Normal depth of flow (m)
0.0005	0.0095	0.0045
0.0008	0.0125	0.0060
0.0010	0.0165	0.0072
0.0013	0.0205	0.0083
0.0015	0.0235	0.0090
0.0018	0.0210	0.0100
0.0020	0.0235	0.0109
0.0025	0.0250	0.0122
0.0030	0.0290	0.0138
0.0040	0.0350	0.0165

The weir was then tested with some aggregate in the weir as shown in table 4.3 and the two flow regimes were compared to establish what was governing the depth upstream of the weir.

Table 4.3 Measurements of flow through the aggregate filled cage

Q (m^3/s)	Depth upstream of the weir (m)
0.00077	0.0340
0.00100	0.0500
0.00128	0.0650
0.00148	0.0765
0.00157	0.0805
0.00168	0.0850
0.00175	0.0870
0.00183	0.0880
0.00195	0.0900
0.00208	0.0915
0.00223	0.0920
0.00240	0.0935

By comparing the measured values in tables 4.2 and 4.3 the aggregate causes a significant increase in the upstream depth and hence is determining the flow through the weir. Figure 4.3 compares the depth of normal flow to the upstream depth of the water when discharging through the empty weir and the upstream depth of the water when discharging through the aggregate filled porous weir.

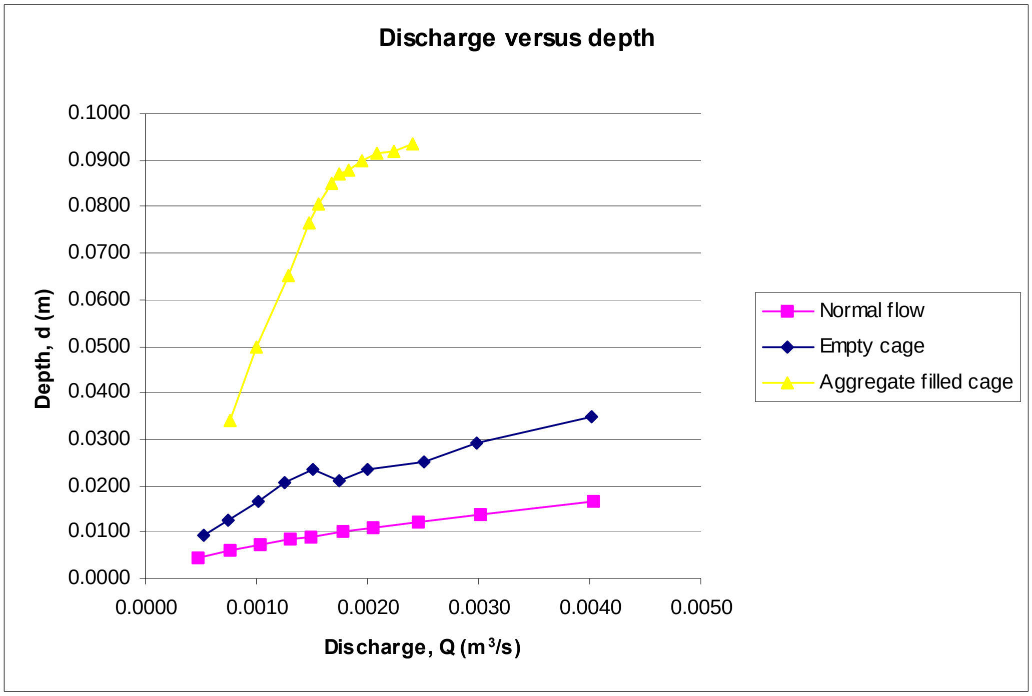

Figure 4.3 Discharge versus depth of flow

Figure 4.3 shows that the empty aggregate cage affects the flow in the wide flume, however its influence is no where near as significant as the flow through the aggregate filled cage.

Once it was established that the porous media would control the flow through the weir, the porous weir was then subjected to a full range of flows. The total flows, including flow through the weir and overflow, ranged from 45L/min to 259L/min.

The following figures 4.4, 4.5 and 4.6 show the locations where the measurements were taken, corresponding to the phase of flow, to obtain data for the analysis.

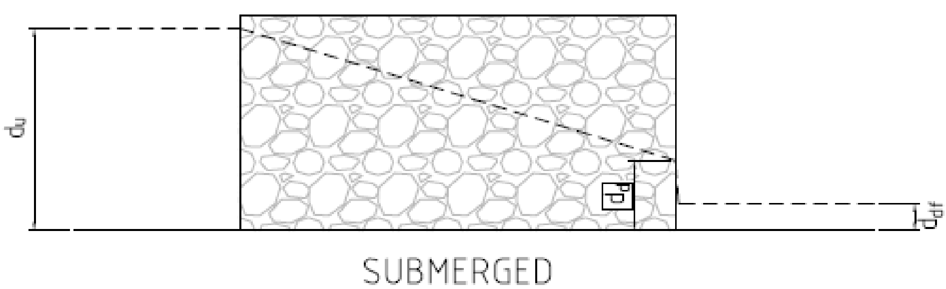

Figure 4.4 Locations of measurements taken during submerged flow

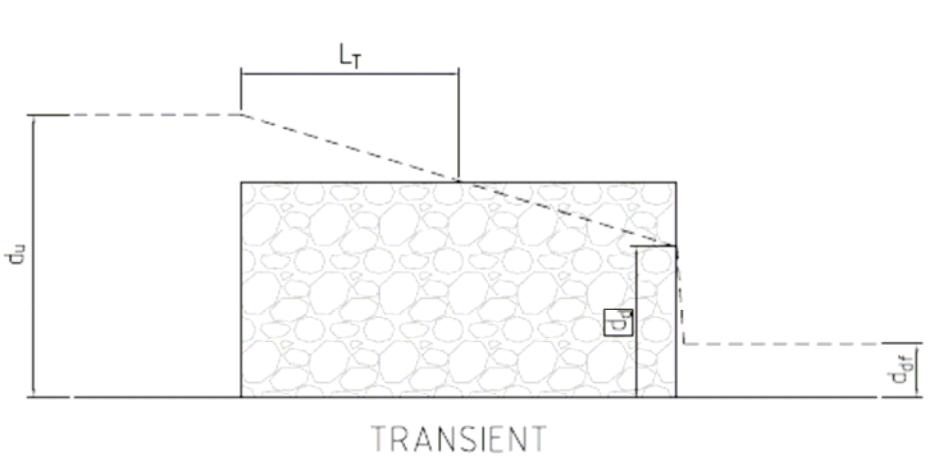

Figure 4.5 Locations of measurements taken during transient flow

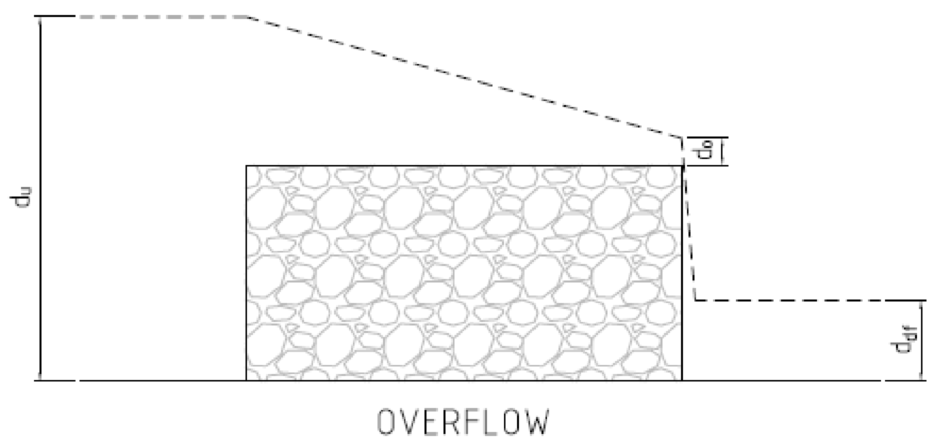

Figure 4.6 Locations of measurements taken during overflow

The upstream depth, d_u, was measured approximately 200mm upstream of the weir and central to the wide flume. This measurement was taken to show the depth of storage the weir was capable of detaining. This measurement was also used to calculate the upstream head generating the flow through the weir.

When the weir had part of the flow entering through the top of the weir, but none actually overflowing the weir (total discharge of 93 – 185L/min), a measurement was taken of the length of the top of the weir submerged (L_T, figure 4.5). This measured value showed some variability across the top of the weir and as for this reason three measurements of this value were taken and then averaged to define the value. The lateral locations where these measurements were taken are shown as 1, 2 and 3 in figure 4.7.

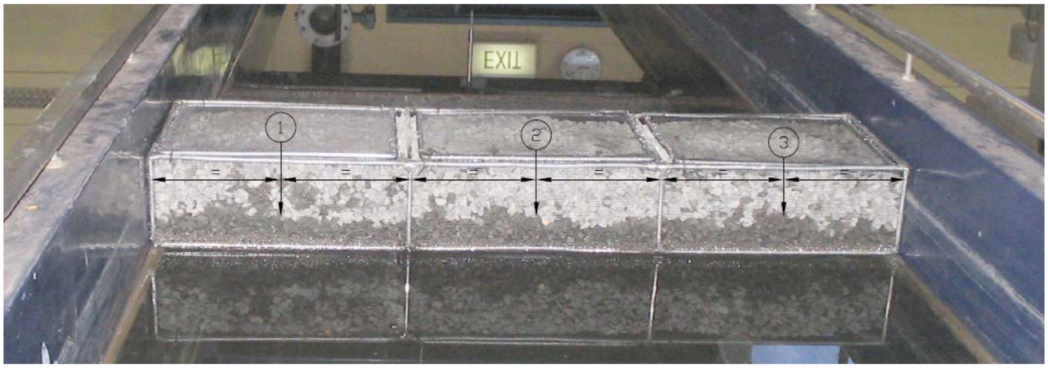

Figure 4.7 Locations of lateral measurements taken across the weir

The depth of flow was measured as it exited the weir (d_d). Measuring this value allowed the head of the flow exiting the weir to be calculated and also gave an indication of the profile of the flow through the weir. This measurement was taken at three locations across the face of the weir in order to obtain an average depth. This was done as a small amount of variability was shown across the face of the weir. Figure 4.7 above shows that quite a significant variation in the depth of discharge is shown across the front of the weir. This figure is not representative of the discharge leaving the weir and only shows that some of the aggregate has absorbed some moisture. The measurements taken in table 4.4 show that the much of the variation in this measurement is less than 5mm, less than the diameter of the aggregate, and is not considered to be sufficient to affect the validity of the model.

The final measurement taken in all flow regimes was of the depth of the downstream flow, d_{df}. This measurement was taken approximately 200mm downstream of the face of the weir and is used to calculate the head of the flow downstream of the weir.

When the weir was experiencing overflow, a measurement was taken at the downstream face. This measurement is shown as d_o and represents the depth of the overflow that is completely unaffected by the porous media as it does not flow through any of it.

The measurements taken during the testing of the porous weir are as shown below in table 4.4.

Table 4.4 Measured values for all phases of flow

Q (L/min)	d_u (mm)	L_T (mm)			d_d (mm)			d_{df} (mm)	d_o (mm)
		Location (see figure 4.7)			Location (figure 4.7)				
		1	2	3	1	2	3		
45	31	-	-	-	9	11	9	6	-
53	42	-	-	-	10	12	9	6.5	-
61	50	-	-	-	12	15	13	7	-
65	56	-	-	-	23	22	22	8.5	-
70	61	-	-	-	23	23	22	9	-
80	69	-	-	-	25	23	25	9	-
87	75.5	-	-	-	26	27	28	10	-
93	80	-	-	-	32	30	30	10	-
103	86	40	60	55	34.0	30.0	33.0	10.5	-
114	90	77	82	90	36.0	40.0	39.0	12.5	-
120	90	85	90	95	42.0	44.0	43.0	13.0	-
134	92	105	119	115	51.0	55.0	51.0	15.0	-
147	94	120	128	120	57.0	64.0	67.0	15.0	-
173	97	135	150	130	75.0	80.0	73.0	15.0	-
185	98	-	-	-	-	-	-	7	0
201	99	-	-	-	-	-	-	7.5	1
234	102	-	-	-	-	-	-	8	2
259	103	-	-	-	-	-	-	8	3

Figure 4.8 shows the relationship between the upstream depth and the discharge for the entire range of flows. This figure shows that when the depth of flow exceeds the height of the upstream face of the weir, a small increase in depth results in a significant increase in discharge.

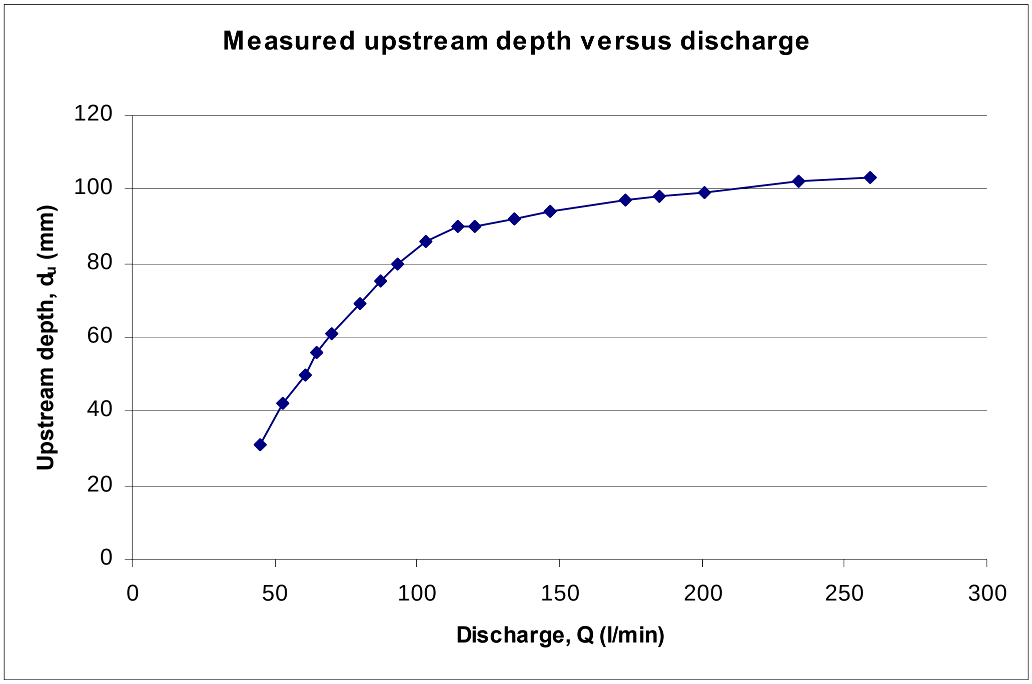

Figure 4.8 Measured upstream depth versus discharge

CHAPTER 5- RESULTS AND DISCUSSION

5.1 Introduction

This chapter is to present and analyse the results and calculations. The analysis is to be undertaken as a one-dimensional analysis. The main objective is to quantify the losses through the weir by analogy to various hydraulic concepts that will be presented in the corresponding section of this chapter.

The results are to be presented according to the three types of flow observed during the testing of the weir.

5.2 Submerged flow analysis

The submerged flow analysis is to be approached by the application of three different equations. The first equation to be used is the Darcy equation. The Darcy equation is traditionally used to estimate seepage flows in soils. The second equation is the Manning's equation and the third is the general equation of gradually varied flow. The Manning equation and general equation of gradually varied flow relate to open channel flow, which is the type of flow experienced through the porous weir.

5.2.1 Submerged flow measurements

The measurements taken that represent the submerged flow through the weir are as shown in table 5.1.

Table 5.1 Submerged flow. Measured values

Q (L/min)	d_u (mm)	d_d (mm)			d_{df} (mm)
		Location (see figure 4.7)			
		1	2	3	
45	31	9	11	9	6
53	42	10	12	9	6.5
61	50	12	15	13	7
65	56	23	22	22	8.5
70	61	23	23	22	9
80	69	25	23	25	9
87	75.5	26	27	28	10
93	80	32	30	30	10

The upstream depth (d_u) influencing the flow through the weir is not equal to that measured. As the base of the weir is made of a 2mm thick impermeable rubber, 2mm needs to be subtracted from the measured upstream depth. Similarly the downstream depth of the discharge exiting the weir needs to have 2mm subtracted from the measured value as the depth measured is relative to the base of the flume and not the base of the porous media in the weir. The rubber mat will reduce the area of the flow due to the reduced depth of flow. The influence of the mat on head loss is considered negligible, as the flow velocity is so small. Three measurements were taken of the downstream depth of discharge (d_d) from the weir, as there was some variability in the depth across the downstream face. These measurements were averaged over the width of the weir to determine a single depth at this location to be used in the analysis. The measured depth of the flow in the flume downstream of the weir (d_{df}) will remain unchanged.

Table 5.2 shows the corrected values to be used in the calculations and Figure 5.1 shows the relationship between the depth at the measured locations and the discharge for the submerged flows.

Table 5.2 Submerged flow. Adjusted measurements

Q (L/min)	d_u (mm)	d_d (mm)	d_{df} (mm)
45	29	7.7	6
53	40	8.3	6.5
61	48	11.3	7
65	54	20.3	8.5
70	59	20.7	9
80	67	22.3	9
87	73.5	25.0	10
93	78	28.7	10

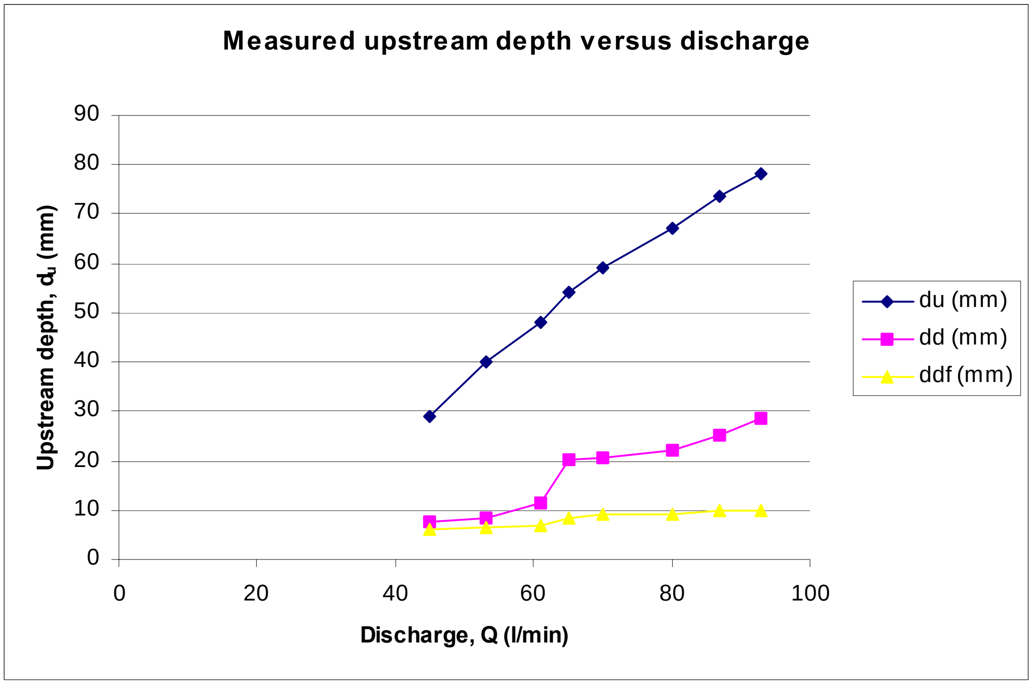

Figure 5.1 Submerged flow. Depth versus discharge

The velocity and cross sectional area of flow to be used in the analysis are to be equal to the measured and calculated values upstream of the weir (denoted by the subscript u). These values are to be used as it is assumed that these values will better represent the majority of the actual flow through the weir. The basis for this assumption stems from the way flow nets are constructed for flow through dams. That is, the flow lines enter the upstream face of the weir perpendicular to the upstream face of the weir. Figure 5.2 shows the authors opinion of the profile of the free surface through the weir.

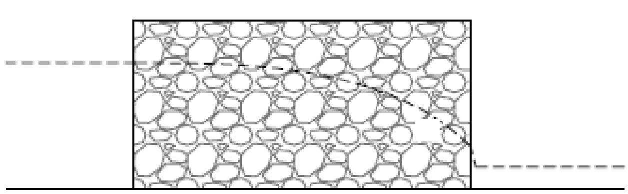

Figure 5.2 Assumed water surface profile through the porous weir

5.2.2 Establishing the type of flow – Turbulent or Laminar

To determine whether the flow is turbulent or laminar, Reynolds number needs to be calculated.

In pipe flow the flow regime is commonly defined by Reynolds number. Reynolds numbers less than 2100 represent laminar flow and Reynolds numbers greater than 4000 represent turbulent flow. The problem with relating the flow through a porous weir to the case of pipes flowing full, is that when pipes are flowing full the flow is steady uniform. In the case of flow through the porous weir the flow is steady non-uniform as for a given discharge the corresponding area and velocity vary with respect to a position in the weir. Therefore the Reynolds numbers associated with pipe flow cannot be directly compared to porous media flow even though they are calculated using the same equation.

Comparison of Reynolds numbers calculated for the flow through the porous weir will be compared to other calculated Reynolds numbers for porous media flow. Calculation of Reynolds number for porous media flow has been widely observed as shown in the literature review. Generally the velocity adopted in the calculation of Reynolds number, in porous media flow, is the macroscopic velocity as it is easily calculated from the bulk cross sectional area of flow. Also the characteristic length adopted is representative of the size of the porous media.

The calculation method as adopted by Bear (1988) will be used to define the flow regime. The equation used is as follows,

$$\mathrm{Re} = \frac{V \times d_{50}}{\nu},$$

…Equation 5.1

Figure 5.3 is presented by Bear and shows generally the laminar, transitional and turbulent regions. If it is compared to the Moody diagram (figure 5.4) it can be seen that there is a similarity between the two and, which is when the flow is turbulent the friction factor tends to a constant value. The graph showing the individual data sets (presented in Bear, 1988) shows the friction factor in the transitional and turbulent regions is slightly more varied than shown above. This may indicate that, like the Moody diagram, when pipe flow is turbulent the friction factor is completely dependant on the roughness of the flow path.

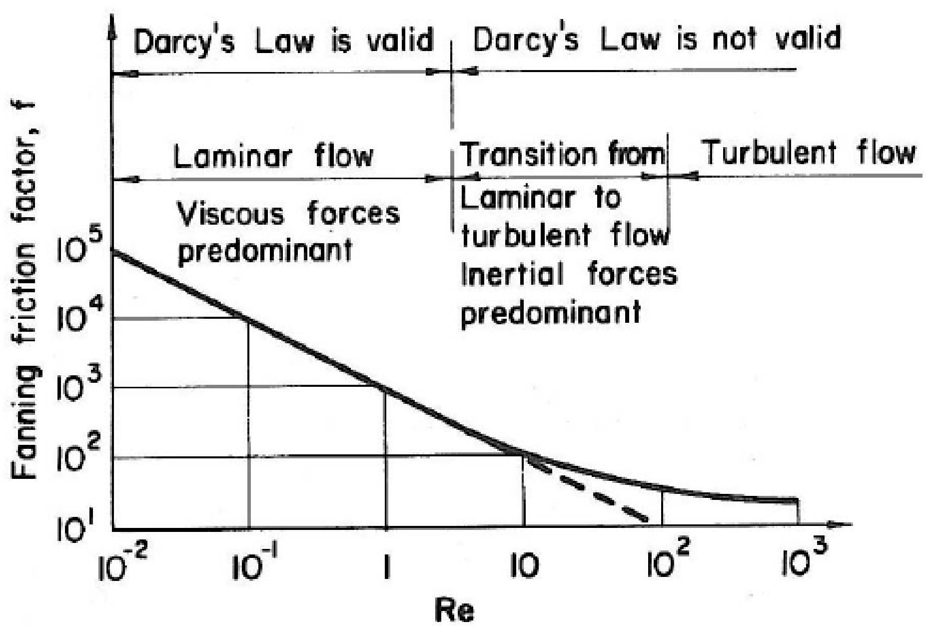

Figure 5.3 Fanning friction factor versus Reynolds number diagram as presented in Bear (1988) for quick reference

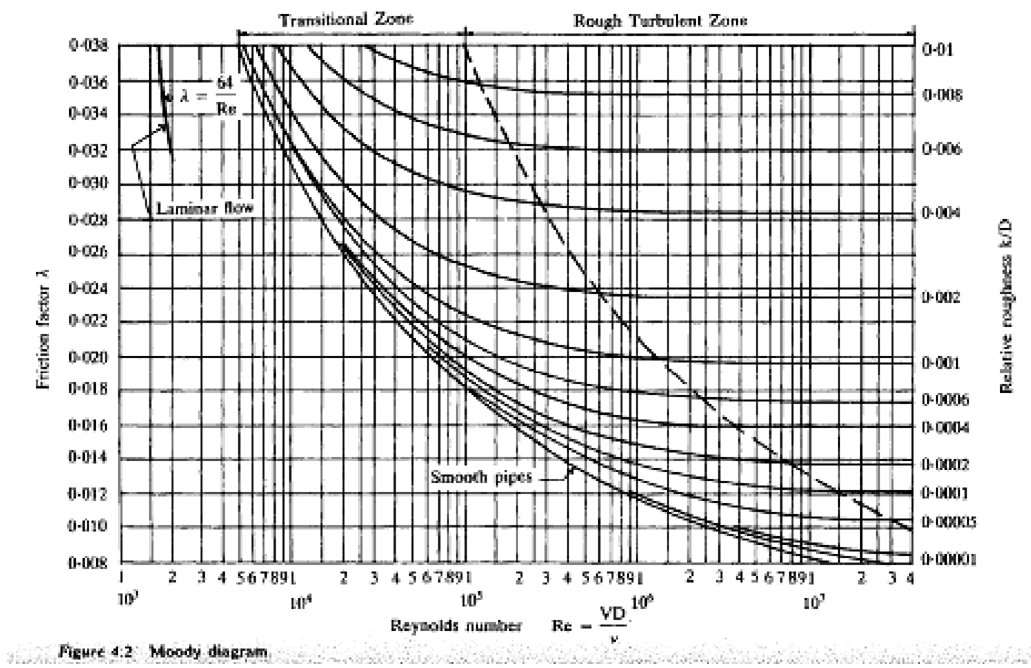

Figure 5.4 Moody diagram from Featherstone and Nalluri (1994)

The calculation of Reynolds number with respect the porous weir tested is shown in table 5.3. The equation used is the same as that presented by Bear (Equation 5.3).

Table 5.3 Submerged flow. Reynolds numbers based on formula presented in Bear (1988)

	Upstream face of weir			Downstream face of weir		
Q (m^3/s)	**A_u (m^2)**	**V_u (m/s)**	**Re**	**A_d (m^2)**	**V_d (m/s)**	**Re**
0.00075	0.0177	0.0424	243	0.0047	0.1604	918
0.00088	0.0244	0.0362	207	0.0051	0.1738	995
0.00102	0.0293	0.0347	199	0.0069	0.1471	842
0.00108	0.0329	0.0329	188	0.0124	0.0873	500
0.00117	0.0360	0.0324	186	0.0126	0.0925	530
0.00133	0.0409	0.0326	187	0.0136	0.0979	560
0.00145	0.0448	0.0323	185	0.0153	0.0951	544
0.00155	0.0476	0.0326	187	0.0175	0.0886	507

Table 5.3 presents the calculated values of Reynolds number achieved by the submerged flow through the weir. These Reynolds numbers show the minimum (upstream face) and the maximum (downstream face) values of Reynolds achieved for the flow through the weir.

The values of Reynolds number, as shown above in table 5.3, appear well into the turbulent zone when compared to figure 5.3 In figure 5.3 and reported by Bear (1988), the onset of turbulent flow is approximately Reynolds number of 100.

This is also supported by the results presented by Venkataraman and Rama Mohan Rao (1998) in figure 2.1. In this case the corresponding characteristic length is represented by the square root of intrinsic permeability. The permeability of the material used in the model porous weir was not measured although similar materials (particle diameter and porosity) presented by Venkataraman and Rama Mohan Rao (1998) show an intrinsic permeability of 0.0001cm^2 (coefficient of permeability of 0.0981m/s) for similar porous media. Figure 5.5 below is another source indicating the range of permeability corresponding to the type of porous media. It shows that the permeability adopted is within the range expected for gravels.

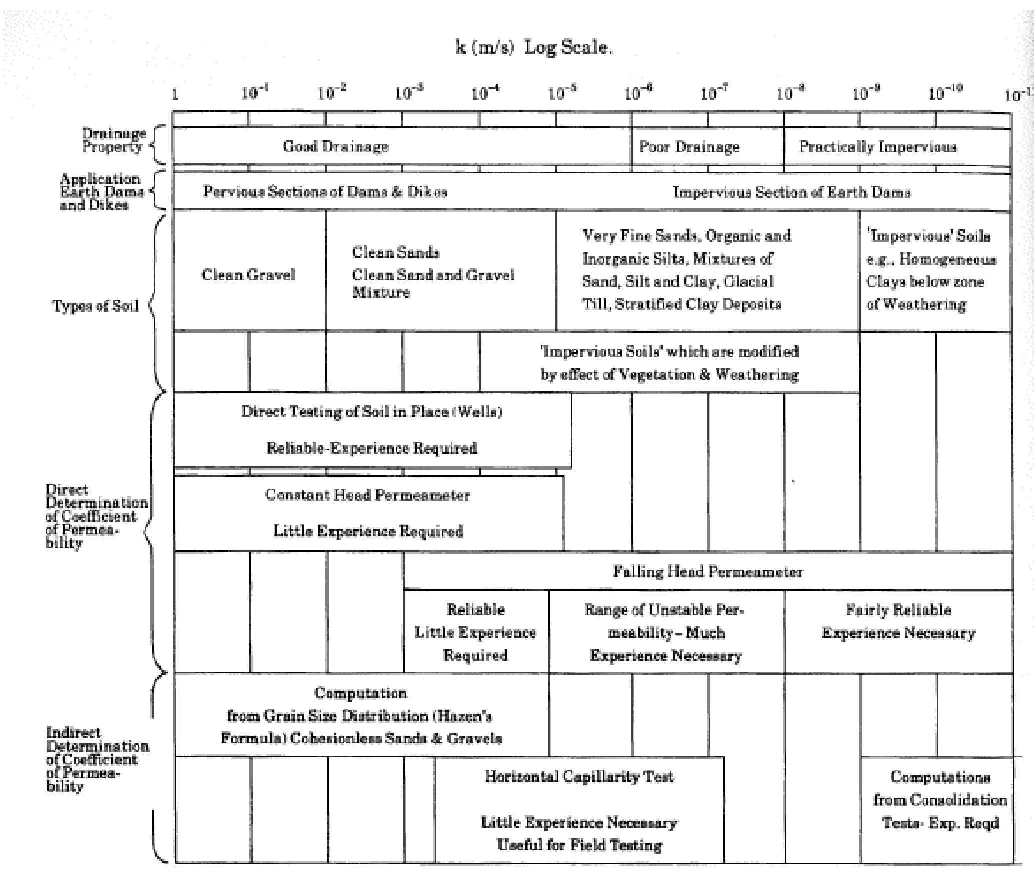

Figure 5.5 Coefficient of permeability corresponding to various types of soil

The intrinsic permeability of 0.0001cm^2 has been adopted for use, to compare Reynolds numbers in the literature to those associated with the porous weir. The Reynolds numbers calculated using the method proposed by Venkataraman and Rama Mohan Rao (1998) are shown in table 5.4.

Table 5.4 Submerged flow. Reynolds numbers based on formula by Venkataraman and Rama Mohan Rao

	Upstream face of weir			Downstream face of weir		
Q (m^3/s)	**A_u (m^2)**	**V_u (m/s)**	**Re**	**A_d (m^2)**	**V_d (m/s)**	**Re**
0.00075	0.0177	0.0424	424	0.0047	0.1604	1604
0.00088	0.0244	0.0362	362	0.0051	0.1738	1738
0.00102	0.0293	0.0347	347	0.0069	0.1471	1471
0.00108	0.0329	0.0329	329	0.0124	0.0873	873
0.00117	0.0360	0.0324	324	0.0126	0.0925	925
0.00133	0.0409	0.0326	326	0.0136	0.0979	979
0.00145	0.0448	0.0323	323	0.0153	0.0951	951
0.00155	0.0476	0.0326	326	0.0175	0.0886	886

The Reynolds numbers in table 5.4, when compared to those in figure 2.1, show the flow is in the turbulent region.

The differences in the Reynolds numbers calculated by the method presented by Bear and the method proposed by Venkataraman and Rama Mohan Rao is due to the different characteristic lengths used in the calculations. Both calculations were performed to compare the flow to two different sets of results presented by these authors. Both lead to the conclusion that the flow through the weir is turbulent.

5.2.3 Initial development

In all equations to be used in the analysis the head at key locations is critical in finding a relationship between the discharge and the porous media. Therefore the analysis will begin with calculations of head (energy) at the locations where measurements were taken. The calculations of the head at these locations were based on the following equation. This is simply Bernoulli's energy equation when applied to open channels and it defines the specific energy at a given location.

$$H = y + \frac{V^2}{2 \times g},$$

…Equation 5.2

Table 5.5 shows the head calculated for the corresponding discharge at the three locations where measurements were taken. The head upstream of the weir (H_u) is calculated from the measured depth of the flow and the velocity of the flow upstream of the weir. The calculated head at this location is approximately equal to the depth of the flow at the given location due to the velocity component being so small. The velocity component of the head in this region is equal to less than the accuracy to which the depth of the flow could be measured (±0.0005m) and for this reason will be ignored in the calculation of the total head at this location.

Table 5.5 Submerged flow. Head calculated at various locations based on depth and velocity

Q (m^3/s)	H_u (m)	H_d (m)	H_{df} (m)
0.00075	0.0290	0.0090	0.0081
0.00088	0.0400	0.0099	0.0090
0.00102	0.0480	0.0124	0.0099
0.00108	0.0540	0.0207	0.0107
0.00117	0.0590	0.0211	0.0113
0.00133	0.0670	0.0228	0.0120
0.00145	0.0735	0.0255	0.0129
0.00155	0.0780	0.0291	0.0133

It is assumed that the depth of flow entering the weir is equal to that measured at d_u (see figure 4.4). Therefore the head calculated upon entry to the weir is equal to H_u as the actual velocity at d_u is equal to the macroscopic velocity upon entry to the weir.

The head calculated at the downstream face of the weir, H_d, is based on equation 5.2. The depth of discharge from the downstream face of the weir and the macroscopic velocity at that location are used in the calculation. Therefore the head of the flow entering the upstream face and exiting the downstream face of the weir can be compared as they are both based on the macroscopic velocity.

The head of the flow downstream of the weir (H_{df}) can also be calculated using Bernoulli's equation where the area used to calculate the velocity is simply the depth multiplied by the width of the flow. The head of the downstream flow can only be compared to the head upstream of the weir as both of these calculations are based on the actual velocity of flow. The head of the downstream flow cannot be compared to the head at the downstream face of the weir as the head of the downstream flow is calculated based on the actual velocity of the flow and the head at the downstream face of the weir is based on the macroscopic velocity.

Figure 5.6 shows the difference between the head upstream of the weir (H_u) and the head of the flow downstream of the weir (H_{df}). The difference between the two plots represents the head loss across the weir.

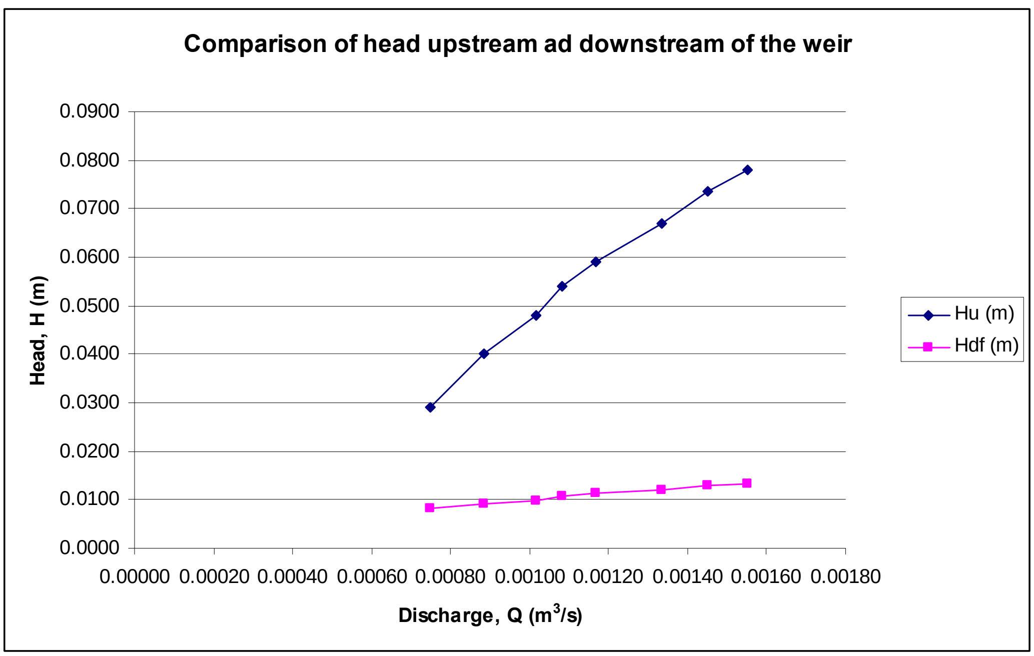

Figure 5.6 Submerged flow. Comparison of head upstream and downstream of the weir

From here on the only values of head to be used in the calculations will be the head upstream of the weir and the head of the downstream flow. This is because these two quantities accurately represent the head at these two locations and they together can be used to represent the total head loss across the weir structure.

5.2.4 Application of the Darcy equation

The Darcy equation is used in seepage flow problems where the flow paths are very small and the flow is laminar. The flow has been shown to be turbulent, however this equation will be investigated in order to rule out laminar flow and the application of the traditional Darcy equation. The measured and calculated data will then be applied to some of the variations to the Darcy equation that have been reported to account for the turbulent flow.

5.2.4.1 Darcy equation

The Darcy equation is presented in the literature review as equation 2.5 and is often written as;

$$V = k \times i$$

…Equation 5.3

where;

$$i = \frac{h_L}{L}$$

Table 5.6 shows the calculation of the hydraulic gradient across the weir using the head calculated upstream of the weir and the head of the flow downstream of the weir.

Table 5.6 Submerged flow. Calculation of head loss across the porous weir

Q (m^3/s)	H_u (m)	H_{df} (m)	h_L (m)	i (m/m)
0.00075	0.0290	0.0081	0.0209	0.1304
0.00088	0.0400	0.0090	0.0310	0.1936
0.00102	0.0480	0.0099	0.0381	0.2382
0.00108	0.0540	0.0107	0.0433	0.2705
0.00117	0.0590	0.0113	0.0477	0.2981
0.00133	0.0670	0.0120	0.0550	0.3437
0.00145	0.0735	0.0129	0.0606	0.3789
0.00155	0.0780	0.0133	0.0647	0.4044

In table 5.6 the hydraulic gradient is shown to increase as the head difference between the upstream and downstream faces increases.

The components of the Darcy equation that been calculated are the velocity and the hydraulic gradient. The coefficient of permeability can now be calculated and the values are shown in table 5.7.

Table 5.7 Calculation of the coefficient of permeability

Q (m^3/s)	V_u (m/s)	i (m/m)	k (m/s)
0.00075	0.0424	0.1304	0.3252
0.00088	0.0362	0.1936	0.1870
0.00102	0.0347	0.2382	0.1458
0.00108	0.0329	0.2705	0.1216
0.00117	0.0324	0.2981	0.1087
0.00133	0.0326	0.3437	0.0949
0.00145	0.0323	0.3789	0.0854
0.00155	0.0326	0.4044	0.0805

The calculations in the table above show that the coefficient of permeability is not constant. This cannot be the case as the coefficient of permeability is a constant representing the frictional drag on the porous media caused by the fluid (Fair, 2004). This indicates that the flow is not laminar and the basic Darcy equation is not valid. This is shown in figure 5.7 below where the velocities of the flow calculated above are far greater than those defined as the limit of laminar flow for Darcy's Law.

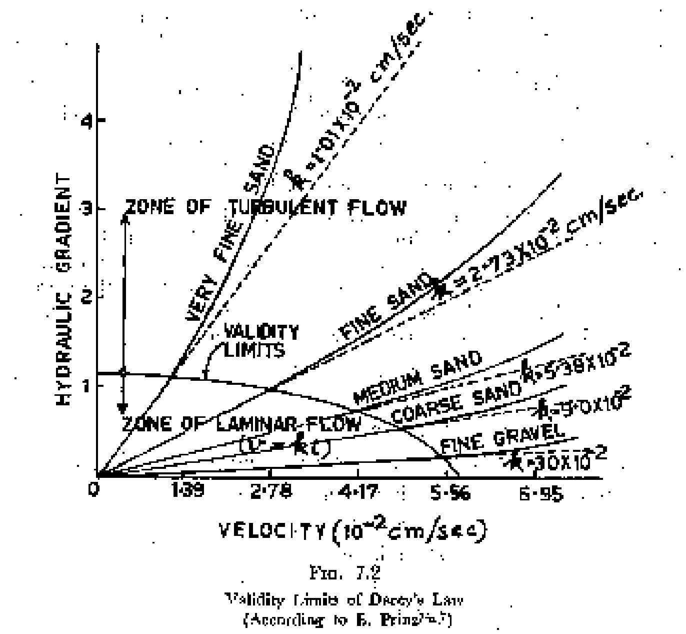

Figure 5.7 Limits of validity for the application of Darcy's equation (Singh, 1967)

5.2.4.2 Modified Darcy equations

To quantify the turbulent flow through the porous media, Singh (1967) presents a modified Darcy equation. The equation is of the form;

$$Q = k \times (i)^n \times A$$

…Equation 5.4

By applying the measured and calculated data for the porous weir to the above formula, the following values for the power, *n*, are calculated.

Table 5.8 Calculations of the modified Darcy equation as presented by Singh (1967)

Q (m^3/s)	k (m/s)	i (m/m)	A_u (m^2)	n
0.00075	0.0981	0.1304	0.0177	0.4118
0.00088	0.0981	0.1936	0.0244	0.6071
0.00102	0.0981	0.2382	0.0293	0.7239
0.00108	0.0981	0.2705	0.0329	0.8358
0.00117	0.0981	0.2981	0.0360	0.9149
0.00133	0.0981	0.3437	0.0409	1.0309
0.00145	0.0981	0.3789	0.0448	1.1433
0.00155	0.0981	0.4044	0.0476	1.2177

Singh reports that n should return a constant value of approximately 0.65. The calculated value is not 0.65 and is not constant, therefore does not apply well to the flow through the porous weir.

Another Darcy type equation (incorporating equations 2.5 and 2.14) is proposed by Missbach and is of the form;

$$Q = k \times i \times A$$

where;

$$i = C \times V^m$$

However, equations that attempt to define the hydraulic gradient will not work, as the value of the hydraulic gradient is known from measurements taken during the experimental work. This type of equation is simply the original Darcy equation, which has been shown not to apply in section 5.3.3.1.

5.2.5 Application of Manning's equation

Open channel flow is the flow experienced when the water surface is exposed to the atmosphere and is at atmospheric pressure. The flow through the weir is considered to be open channel flow as the flow is not confined and the water surface is at atmospheric pressure.

Manning's equation is an equation commonly used in open channel flow. Manning's Equation is to be applied to the experimental data to determine if there is a relationship between Manning's equation and the discharge through the weir.

The Manning equation commonly applied to open channel flow and presented in the literature review is (equation 2.31);

$$V = \frac{R^{2/3} S_0^{1/2}}{n}$$

This form of Manning's equation is used in steady uniform flow. In steady uniform flow the friction slope is equal to the bed slope and the bed slope is subsequently substituted into the equation.

As the flow through the weir is not steady uniform flow, the Manning's equation to be used is;

$$V = \frac{R^{2/3} S_f^{1/2}}{n}$$

…Equation 5.5

If we adopt the characteristics of the flow upstream of the weir, we are left with three unknown variables in the equation (R, S_f and n). Of the unknown variables the friction slope can be equated to the head loss across the weir and the hydraulic radius can be calculated from porous media properties, leaving only Manning's n to be determined.

The important value to be determined in the Manning equation is the value of Manning's n. Manning's n is a measure of the frictional resistance of the channel (Chadwick and Morphett p. 124) and is always reported as a constant value for a given surface type. In the case of flow through the porous weir the flow paths through the porous media are representative of the channel.

5.2.5.1 The hydraulic radius

The hydraulic radius is defined as, area of flow divided by the wetted perimeter.

In the case of the porous media the hydraulic radius is not as easily calculated as if the cross section was a simple rectangular or trapezoidal section. The porous media significantly affects the cross sectional area of flow and the wetted perimeter. In determining the value of the hydraulic radius, several assumptions were made. It is assumed that, the particles are of spherical shape with a diameter 5.725mm, the packing of the individual particles of the porous media is uniform throughout the weir and the porosity (*n*), although a volumetric measure, is representative of the ratio of area of void to area of solid taken through a typical cross section.

Based on these assumptions the hydraulic radius of flow through the weir can be determined. The cross sectional area of flow is equal to,

$$A = d_u \times w \times n$$

The wetted perimeter is determined by

$$P = N \times \pi d_{50}$$

N is the equivalent number of full particles in a typical cross section. *N* is equal to, the total area of solid through a cross section, divided by the cross sectional area of one particle.

$$N = \frac{d_u w - (d_u w) n}{\left(\frac{\pi d_{50}^2}{4}\right)}$$

$$P = \frac{d_u w - (d_u w)n}{\left(\frac{\pi d_{50}^2}{4}\right)} \times \pi d_{50}$$

$$P = \frac{4(d_u w)(1-n)}{d_{50}}$$

$$R = \frac{A}{P}$$

$$R = \frac{d_{50} n}{4(1-n)}$$

…Equation 5.6

This equation shows that the hydraulic radius is not dependent on the depth of the flow, as is usually found when calculated in a simple rectangular or trapezoidal section, and is dependent on the particle size and the porosity of the porous media. Table 5.9 shows that all the variables for each discharge through the weir are constant and therefore as the discharge increases the hydraulic radius for flow through the weir remains a constant value.

Table 5.9 Hydraulic radius calculations

Q (m^3/s)	d_{50} (m)	n%	R (m)
0.00075	0.005725	37.66	0.000865
0.00088	0.005725	37.66	0.000865
0.00102	0.005725	37.66	0.000865
0.00108	0.005725	37.66	0.000865
0.00117	0.005725	37.66	0.000865
0.00133	0.005725	37.66	0.000865
0.00145	0.005725	37.66	0.000865
0.00155	0.005725	37.66	0.000865

5.2.5.2 The friction slope

Table 5.10 shows the calculated head loss and friction slope across the weir for the corresponding discharges. The head upstream of the weir and the head of the downstream flow are used to calculate the head loss across the weir.

Table 5.10 Head loss and friction slope

Q (m^3/s)	h_L (m)	S_f (m/m)
0.00075	0.0209	0.1304
0.00088	0.0310	0.1936
0.00102	0.0381	0.2382
0.00108	0.0433	0.2705
0.00117	0.0477	0.2981
0.00133	0.0550	0.3437
0.00145	0.0606	0.3789
0.00155	0.0647	0.4044

Table 5.10 shows that the friction slope increases as the discharge increases.

5.2.5.3 Analogy to open channel flow

Table 5.11 shows the characteristics of Manning's equation when applied to steady uniform open channel flow and compared to the flow characteristics of the flow through the porous weir.

Table 5.11 Comparison of the characteristics of steady uniform open channel flow and the flow through the porous weir

As discharge increases:	
Steady uniform open channel flow	**Flow through porous weir**
▪ A increases	▪ A increases
▪ R increases	▪ R is constant
▪ *n* is constant	▪ *n* is constant
▪ $S_f = S_0$	▪ $S_f \neq S_0$
▪ S_f is constant	▪ S_f increases
▪ V increases	▪ V is constant

In the steady uniform case we have shown that all components of the Manning's equation are constant except for velocity and the hydraulic radius. Therefore it can be shown that

$$V \propto R^{2/3}$$

In the case of flow through the porous weir, all the variables are constant except for the energy gradient. If Manning's equation is reduced as it was for the steady uniform flow case then

$$V \propto S_f^{1/2}$$

Since the velocity through the porous weir has been shown to be constant (see table 5.4), the energy slope must also be constant. Previous calculations have shown that the energy slope is not constant and as such the Manning's equation is not suitable to be used to define the porous weir flow.

5.2.6 The general equation of gradually varied flow

The general equation of gradually varied flow is an open channel flow equation that is applied to non-uniform flow.

The flow through the porous weir is non-uniform as the water surface profile varies along the length of flow through the weir. This is shown by the difference in the upstream and downstream depths of flow.

Varied flow can be classified into two different types that are analysed using different principles. The first is rapidly varied flow and is analysed by balancing specific energy and momentum at a point upstream and downstream of a structure. The second is gradually varied flow and is analysed by balancing frictional resistance and energy equations (Chadwick and Morfett, 2002).

The porous weir needs to be analysed using gradually varied flow principles. This is because when the fluid passes through the weir there is considerable interaction between the porous media and the fluid causing significant frictional losses.

The general equation for gradually varied flow presented by Chadwick and Morfett (2002 p. 154) is;

$$\frac{dy}{dx} = \frac{S_0 - S_f}{1 - \alpha \dfrac{Q^2 w}{A^3 g}}$$

…Equation 5.7

where;

$\frac{dy}{dx}$ = the slope of the water surface relative to the bed slope.

w = top width of flow

The slope of the water surface is assumed to be equal to the difference between the depth upstream and the downstream depth of flow. The reason for this is the downstream depth of flow can be determined by applying the Manning's equation to the downstream channel conditions. The head loss can be calculated from the difference in head at these two locations.

We know that the friction slope is equal to;

$$S_f = \frac{h_f}{L}$$

and can be calculated from measurements taken during the experimentation.

The head loss due to friction in steady uniform flow can be described by the Darcy-Weisbach equation (below) and is commonly found in non-circular conduit flow problems.

$$h_f = \frac{fLV^2}{8gR}$$

…Equation 5.8

5.2.6.1 Darcy-Weisbach equation

The Darcy-Weisbach equation is usually used for steady uniform pipe flow problems. A comparison between the variables in the pipe flow case will be compared to the same variables in the porous weir case to determine the applicability of the analogy.

Table 5.12 Comparison of the characteristics of steady uniform pipe flow and flow through the porous weir

As discharge (Q) increases:	
Steady uniform pipe flow	**Flow through porous weir**
▪ A is constant	▪ A increases
▪ L is constant	▪ L is constant
▪ R is constant	▪ R is constant
▪ h_f increases	▪ h_f increases
▪ $S_f \neq S_0$	▪ $S_f \neq S_0$
▪ S_f increases	▪ S_f increases
▪ *f* is constant (turbulent flow)	▪ *f* is constant (turbulent flow)
▪ V increases	▪ V is constant

If the variables in table 5.12 are applied to the Darcy-Weisbach equation the steady uniform pipe flow equation reduces to the equation below as all other variables are constants.

$$h_f \propto V^2$$

If the flow through the porous media is applied to the Darcy-Weisbach equation then the same equation can be reached. However in this case the head loss is not constant and the velocity is, therefore the relationship is not valid.

It is noticed that the only other variable that increases as the discharge increases is the cross sectional area of flow. It is therefore proposed to apply the following formula to the porous weir flow.

$$h_f \propto A$$

Table 5.13 below shows the relationship between the head loss and the cross sectional area of flow.

Table 5.13 Submerged flow. Head loss and cross sectional area

Q (m^3/s)	A_u (m^2)	h_L (m)
0.00075	0.0177	0.0209
0.00088	0.0244	0.0310
0.00102	0.0293	0.0381
0.00108	0.0329	0.0433
0.00117	0.0360	0.0477
0.00133	0.0409	0.0550
0.00145	0.0448	0.0606
0.00155	0.0476	0.0647

Figure 5.8 also shows the relationship.

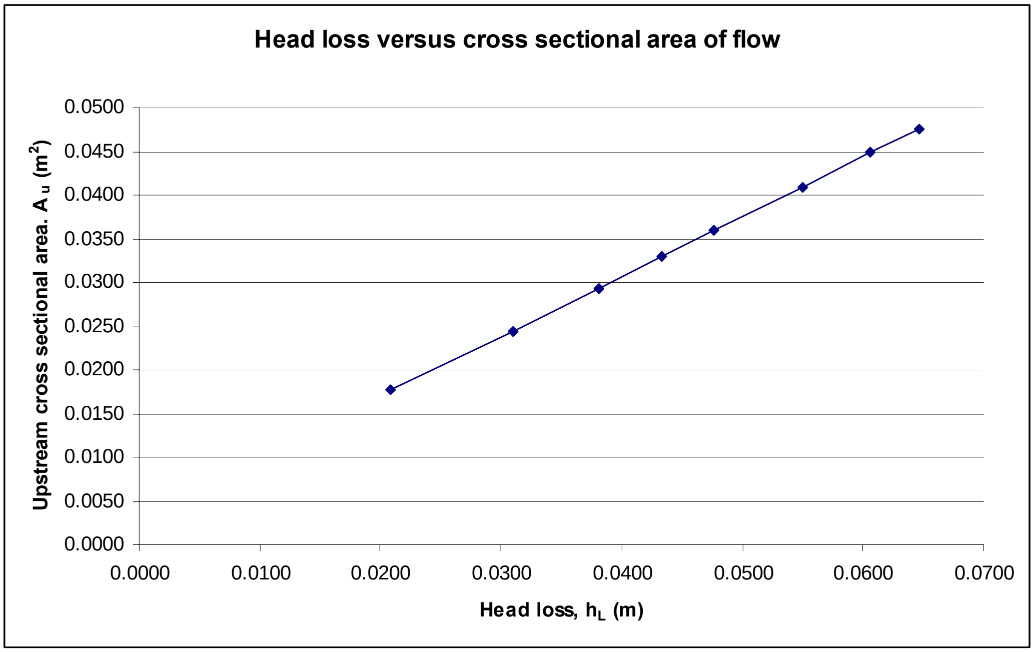

Figure 5.8 Submerged flow. Head loss versus cross sectional area of flow

The equation for the energy gradient is then equal to

$$S_f = \frac{h_f}{L} \propto \frac{A_u}{L}$$

$$S_f = \frac{f \times A_u}{L}$$

where;

f = a friction factor (m^{-1})

The modified Darcy-Weisbach equation is

$$h_f = f \times A_u$$

…Equation 5.9

We can then substitute the friction slope into the Darcy-Weisbach equation.

$$\frac{dy}{dx} = \frac{S_0 - \frac{fA}{L}}{1 - \alpha \frac{Q^2 w}{A_u^3 g}}$$

$$f = \frac{L}{A_u}\left(S_0 - \frac{dy}{dx}\left(1 - \alpha \frac{Q^2 w}{A_u^3 g}\right)\right)$$

…Equation 5.10

When this equation is applied to the measured values (Q, w, L) and previously calculated values ($\frac{dy}{dx}$, A, S_0) the following values for f are revealed (table 5.14).

Table 5.14 Submerged flow. Calculation of friction factors

Q (m^3/s)	L (m)	A_u (m^2)	S_0 (m/m)	dy/dx	w (m)	f (m^{-1})
0.00075	0.16	0.0177	0.00333	-0.1438	0.61	1.322
0.00088	0.16	0.0244	0.00333	-0.2094	0.61	1.390
0.00102	0.16	0.0293	0.00333	-0.2563	0.61	1.415
0.00108	0.16	0.0329	0.00333	-0.2844	0.61	1.395
0.00117	0.16	0.0360	0.00333	-0.3125	0.61	1.402
0.00133	0.16	0.0409	0.00333	-0.3625	0.61	1.430
0.00145	0.16	0.0448	0.00333	-0.3969	0.61	1.426
0.00155	0.16	0.0476	0.00333	-0.4250	0.61	1.438

The friction factors calculated above represent the friction factors associated with the bulk cross sectional area of flow. These friction factors are shown in figure 5.9.

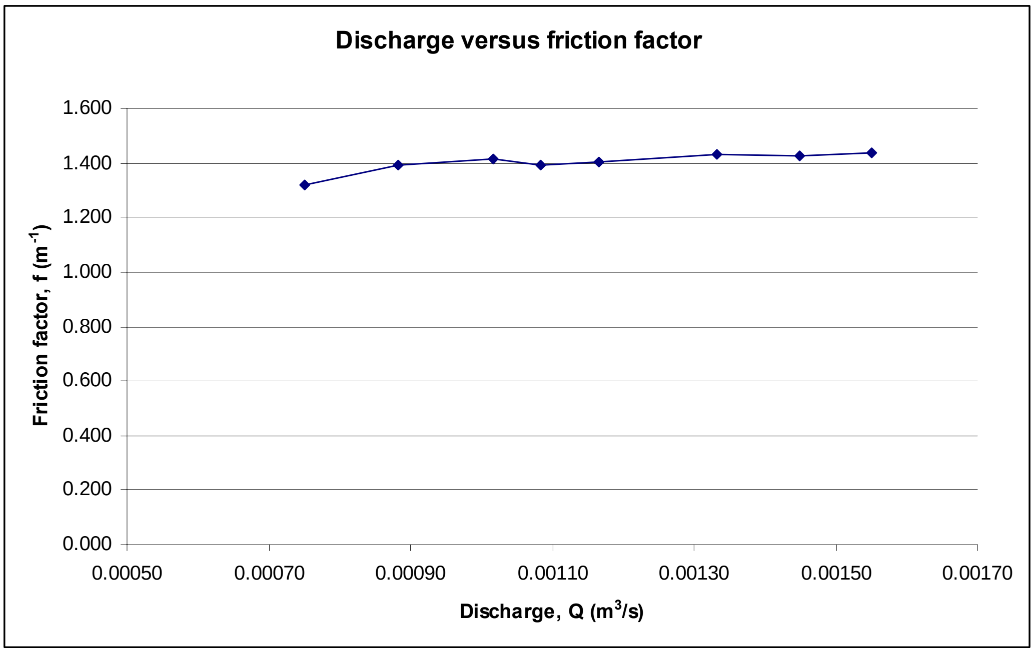

Figure 5.9 Submerged flow. Relationship between friction factor and discharge

These friction factor values determined above are considered to be constant over the submerged range of flows for the weir configuration used in this report. The friction factor values calculated are large compared to traditional friction factor values as the interaction between the porous media and the fluid is much greater than found in traditional pipe flow. The bulk area of flow and the macroscopic velocity are used in the calculations and have also had an influence on the magnitude of friction factor calculated.

In order to check the relationship the theoretical discharge is calculated based on the gradually varied flow equation and the friction factor being equal to 1.418. Table 5.15 and figure 5.10 below show the results.

Table 5.15 Submerged flow. Theoretical calculation of the upstream depth based on the measured depth of flow downstream

Q (m^3/s)	d_{df} (m)	d_u (m)	f (m^{-1})
0.00075	0.0060	0.0410	1.418
0.00088	0.0065	0.0449	1.418
0.00102	0.0070	0.0486	1.418
0.00108	0.0085	0.0596	1.418
0.00117	0.0090	0.0633	1.418
0.00133	0.0090	0.0635	1.418
0.00145	0.0100	0.0709	1.418
0.00155	0.0100	0.0710	1.418

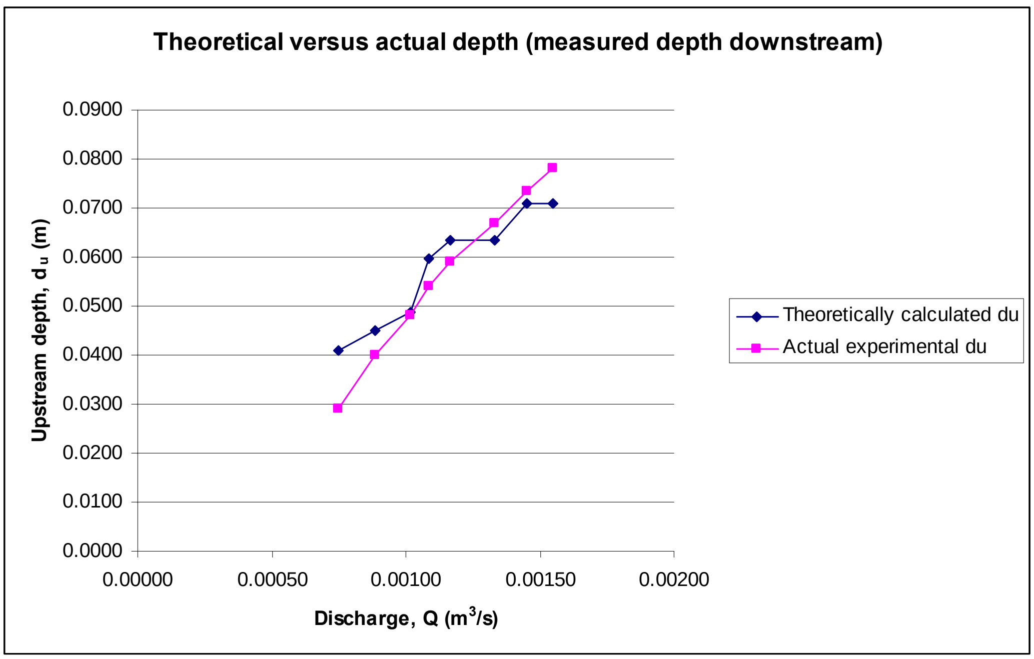

Figure 5.10 Submerged flow. Theoretically calculated depth versus actual experimental depth (measured depth downstream)

The graph (figure 5.10) above does not show a very good correlation between the measured and calculated depths corresponding to the associated discharge. However, if the downstream depths are modified by less than 1mm (which could be error in the readings taken during experimentation) the following correlation is obtained (table 5.16 and figure 5.11).

Table 5.16 Submerged flow. Theoretical calculation of the upstream depth based on the modified depth of flow downstream

Q (m^3/s)	d_{df} (m)	Δ d_{df} (m)	d_u (m)	f (m^{-1})
0.00075	0.0050	-0.0010	0.0340	1.418
0.00088	0.0060	-0.0005	0.0413	1.418
0.00102	0.0070	0.0000	0.0486	1.418
0.00108	0.0080	-0.0005	0.0560	1.418
0.00117	0.0085	-0.0005	0.0598	1.419
0.00133	0.0095	0.0005	0.0670	1.418
0.00145	0.0105	0.0005	0.0745	1.418
0.00155	0.0110	0.0010	0.0782	1.418

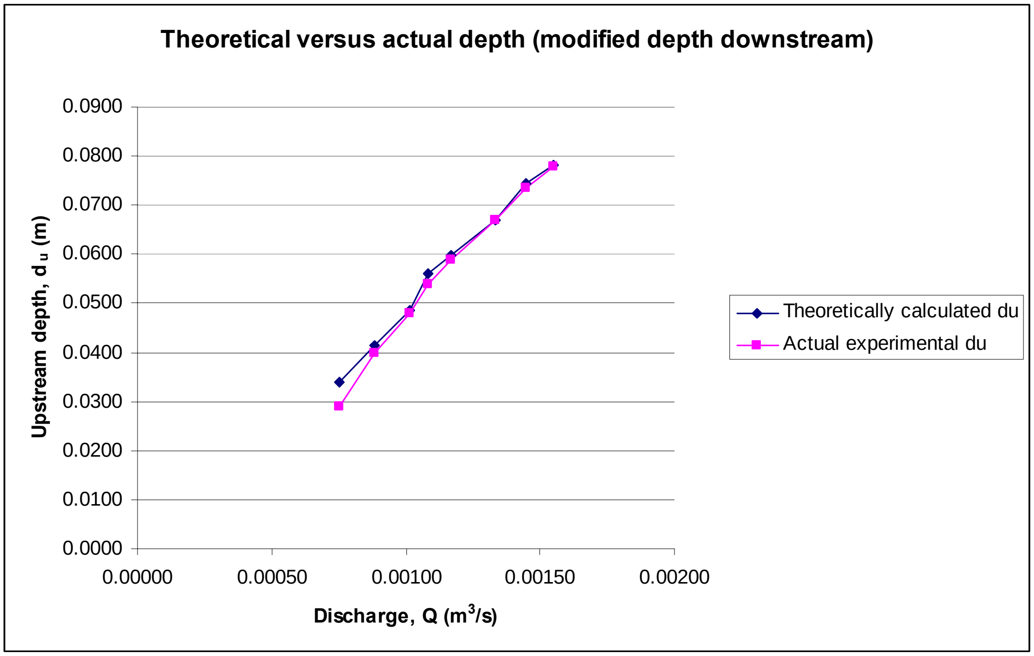

Table 5.11 Submerged flow. Theoretically calculated depth versus actual experimental depth (modified depth downstream)

This formula shows quite a good relationship between discharge and upstream depth. The variation in the theoretical calculations is due to the small errors in the measurement of the downstream depth of flow used in the calculations. The small errors in these measurements have shown to show up as a large difference in the calculation of the corresponding upstream depth. This is due to the small scale of the model.

By using the gradually varied flow equation the upstream depth can now be calculated for a given discharge. Therefore the general equation for gradually varied flow gives the head discharge relationship for the porous weir.

5.3 Transient flow

Transient flow has previously been defined as where the free surface of the flow enters the weir through the top surface of the weir.

The transient flow will be modelled from two different perspectives. As this phase is between the submerged and overflow phases the flow will be modelled from both angles. The first analogy will be to the submerged phase where the weir will be compared to the general equation for gradually varied flow in combination with the modified Darcy-Weisbach equation (equation 5.9). These equations resulted in a good correlation in the submerged phase. The second analogy will be to the general weir equation, which be used in the overflow phase to represent the discharge.

In the transient phase the discharge through the weir increases from 0.00155 to 0.0031m^3/s and a corresponding increase in upstream head from 0.078 to 0.095m.

5.3.1 Transient flow measurements

The measurements taken that represent the transient flows, from the interface of the submerged flow to the interface of the overflow (as shown in figure 2.3), are shown in table 5.17.

Table 5.17 Transient flow. Measured values

		Length over top of weir (mm)			Downstream depth (mm)			
Q (L/min)	d_u (mm)	1	2	3	1	2	3	d_{df} (mm)
93	80	-	-	-	32	30	30	10
103	86	40	60	55	34.0	30.0	33.0	10.5
114	90	77	82	90	36.0	40.0	39.0	12.5
120	90	85	90	95	42.0	44.0	43.0	13.0
134	92	105	119	115	51.0	55.0	51.0	15.0
147	94	120	128	120	57.0	64.0	67.0	15.0
173	97	135	150	130	75.0	80.0	73.0	15.0
185	98	-	-	-	-	-	-	7

The measurements taken for the transient range of flows needs to be processed similar to how the submerged range of flows was in section 5.2.1. Another measurement presented here (not relevant to the submerged range) is the length over the top of the weir. This measurement represents the top length of the weir that is submerged and the position is shown in figure 4.5.

Table 5.18 shows the corrected values to be used in the calculations.

Table 5.18 Transient flow. Adjusted measurements

Q (L/min)	d_u (mm)	L_T (mm)	d_d (mm)	d_{df} (mm)
103	84	51.7	30.3	10.5
114	88	83.0	36.3	12.5
120	88.5	90.0	41.0	13.0
134	90	113.0	50.3	15.0
147	92	122.7	64.0	15.0
173	95	138.3	74.0	15.0

The head upstream is again to be based solely on the depth of the water upstream of the weir (d_u) as the velocity is still has negligible influence on the total H_u.

The calculated head upstream and downstream of the weir is shown in table 5.19.

Table 5.19 Transient flow. Head calculated upstream and downstream of the weir

Q (m^3/s)	H_u (m)	H_{df} (m)
0.00172	0.0840	0.0142
0.00190	0.0880	0.0157
0.00200	0.0885	0.0212
0.00223	0.0900	0.0209
0.00245	0.0920	0.0238
0.00288	0.0950	0.0302

Figure 5.12 shows the information presented in table 5.19. The difference between the two plots represents the head loss across the weir.

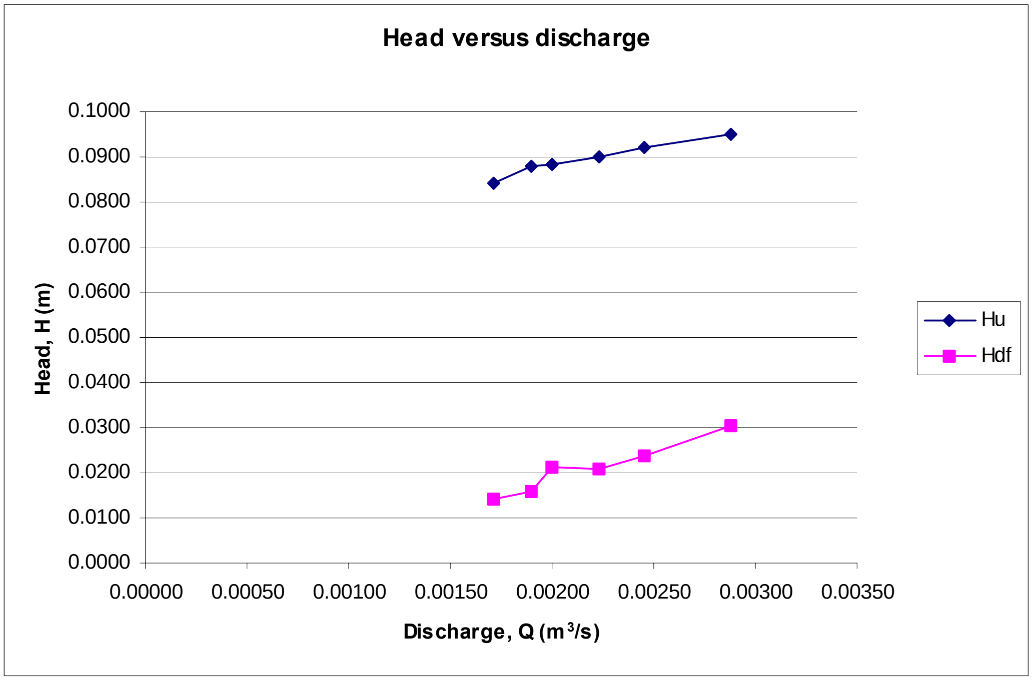

Figure 5.12 Submerged flow. Comparison of head upstream and downstream of the weir

5.3.2 The general equation for gradually varied flow

The development of the equation for gradually varied flow and the Darcy-Weisbach equation was outlined in the analysis of the submerged flow through the porous weir. The same form of the equation will be adopted here. The known variables in the equation are shown in table 5.20.

The calculations of the corresponding friction factors are shown in table 5.20.

Table 5.20 Transient flow. Calculation of friction factors

Q (m^3/s)	L (m)	A_u (m^2)	S_0 (m/m)	dy/dx	w (m)	f (m^{-1})
0.00172	0.16	0.0512	0.00333	-0.4594	0.61	1.443
0.00190	0.16	0.0537	0.00333	-0.4719	0.61	1.414
0.00200	0.16	0.0540	0.00333	-0.5156	0.61	1.536
0.00223	0.16	0.0549	0.00333	-0.5188	0.61	1.519
0.00245	0.16	0.0561	0.00333	-0.5313	0.61	1.521
0.00288	0.16	0.0580	0.00333	-0.5500	0.61	1.524

We can see in table 5.20 that the value of the friction factors calculated are similar to those calculated in the submerged phase although they vary as the discharge increases. This is assumed to be because of errors in the downstream measurements taken during experimentation.

In this phase the friction factor to be adopted, is to be the same as calculated in the submerge flow regime and, is equal to 1.418 and is assumed to be a constant for the media used in the porous weir.

Table 5.21 shows the calculation of the theoretical upstream depth calculated based on a friction factor of 1.418 and the measured downstream depth of flow for the corresponding discharge.

Table 5.21 Transient flow. Theoretical calculation of the upstream depth based on the measured depth of flow downstream

Q (m^3/s)	d_{df} (m)	d_u (m)	f (m^{-1})
0.00172	0.0105	0.0746	1.418
0.00190	0.0125	0.0895	1.418
0.00200	0.0130	0.0930	1.418
0.00223	0.0150	0.1080	1.418
0.00245	0.0150	0.1080	1.418
0.00288	0.0150	0.1085	1.418

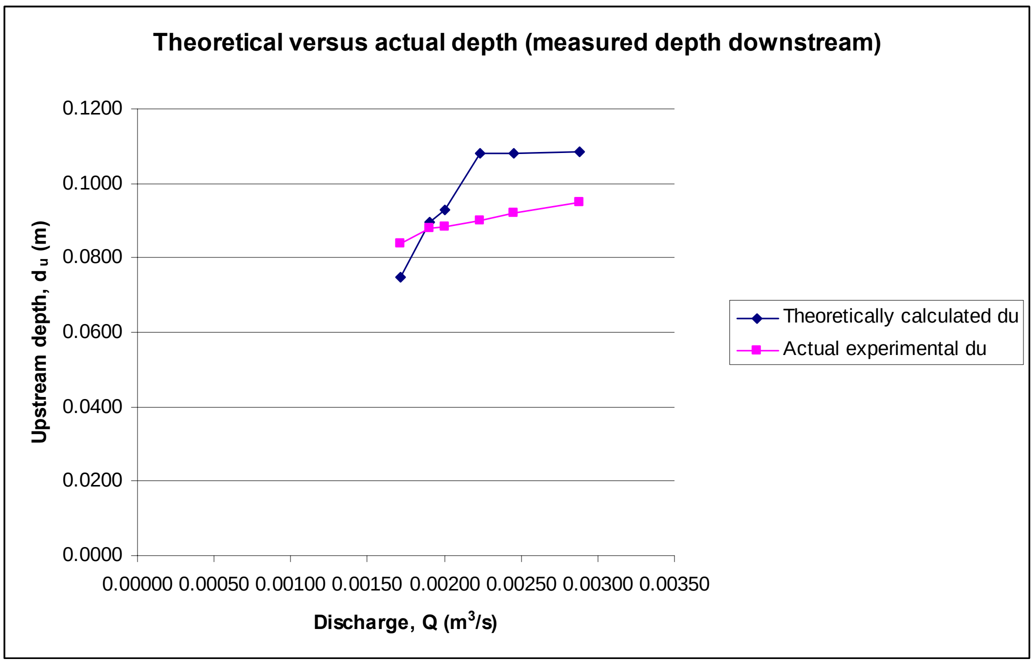

Figure 5.13 Transient flow. Theoretically calculated depth versus actual experimental depth (measured depth downstream)

Figure 5.13 shows the relationship of the calculated depth upstream of the weir based on the measure downstream depth and the discharge. The relationship in figure 5.13 does not appear to be very good.

When the downstream depths of flow are slightly modified (this could be error in the readings taken during experimentation), the following table 5.22 and figure 5.14 show the results.

Table 5.22 Transient flow. Theoretical calculation of the upstream depth based on the modified depth of flow downstream

Q (m^3/s)	d_{df} (m)	Δ d_{df} (m)	d_u (m)	f (m^{-1})
0.00172	0.0115	0.0010	0.0820	1.418
0.00190	0.0120	-0.0005	0.0857	1.418
0.00200	0.0125	-0.0005	0.0895	1.418
0.00223	0.0125	-0.0025	0.0898	1.418
0.00245	0.0130	-0.0020	0.0935	1.418
0.00288	0.0135	-0.0015	0.0975	1.418

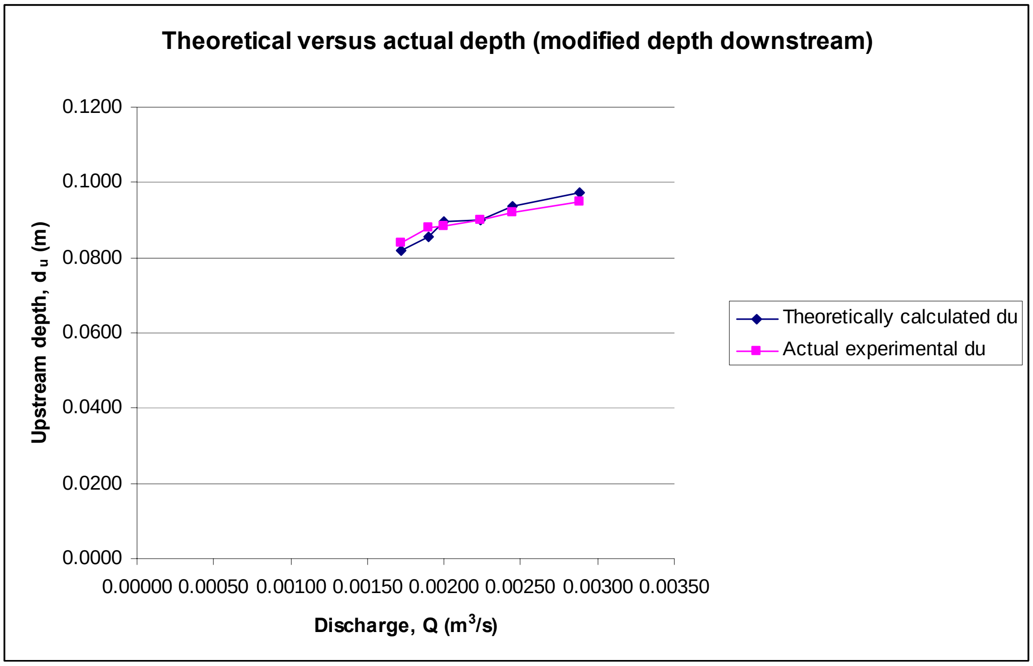

Table 5.14 Transient flow. Theoretically calculated depth versus actual experimental depth (modified depth downstream)

The correlation between the measured and theoretical data is much closer and there may have been some error in the measurement of the depth downstream of the weir. It was noticed during the experimentation that the flow was quite turbulent downstream of the weir, once the discharge exceeded the limit of the submerged phase of flow. The error in the measured depth of flow could be due to the variation in depth of flow across the flume due to the turbulence.

5.3.3 The general weir equation

The general weir equation is as shown below.

$$Q = C \times H^n$$

…Equation 5.11

The data used in the calculation of the transient flow will be calculated based on the quantity of discharge and the head of the flow above that of the submerged flow. This assumes that the submerged component of the discharge remains constant as the head upstream increases. This assumption is assumed valid as in the submerged phase; no increase in the upstream velocity was calculated as the upstream head increased (see table 5.7). The data representing the interface between the submerged and transient phases of flow is shown in the table 5.23.

Table 5.23 Measurements and calculations representing the interface between the submerged and transient flow

Q (m^3/s)	d_u (m)	H_u (m)
0.00155	0.0780	0.0780

The head to be used in the general weir equation is shown in the table 5.24. This data represents the head associated with the increase in flow above that of the flow representing the upper limit of the submerged phase of flow. The head used in the calculation is equivalent to the increase in depth over the upstream face of the weir.

Table 5.24 Transient flow. Discharge and upstream head

Q (m^3/s)	H_u (m)
0.00017	0.0060
0.00035	0.0100
0.00045	0.0105
0.00068	0.0120
0.00090	0.0140
0.00133	0.0170

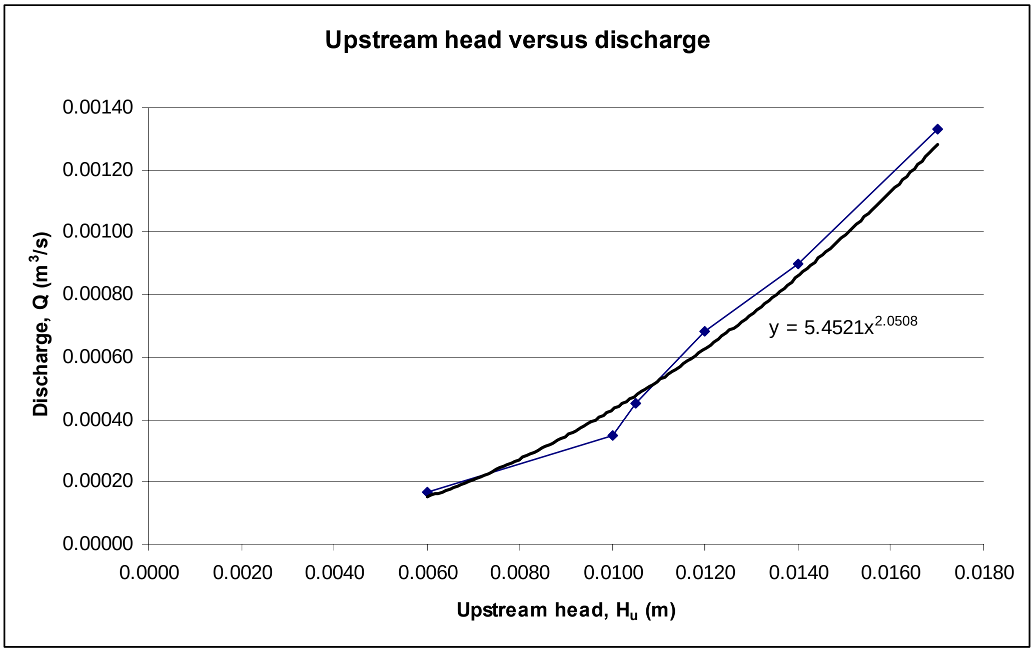

Figure 5.15 Transient flow. Discharge and upstream head

A graph of the head versus discharge is shown in figure 5.15. The trend in the data shows a reasonable fit when the following general weir equation is applied to the data

$$Q = 5.4521 \times H^{2.0508}$$

…Equation 5.12

This equation could be used to represent the transient range of flows. However before a recommendation is made, an attempt will be made to fit a broad crested weir equation to the data.

The weir could be modelled using the ideal broad crested weir equation and applying a coefficient of discharge that varies depending on the head upstream.

$$Q = C_d \times 1.705 \times w \times H^{1.5}$$

…Equation 5.13

The following plot (figure 5.16) shows the ideal broad crested weir (C_d=1) flow compared to the measured flow over the weir.

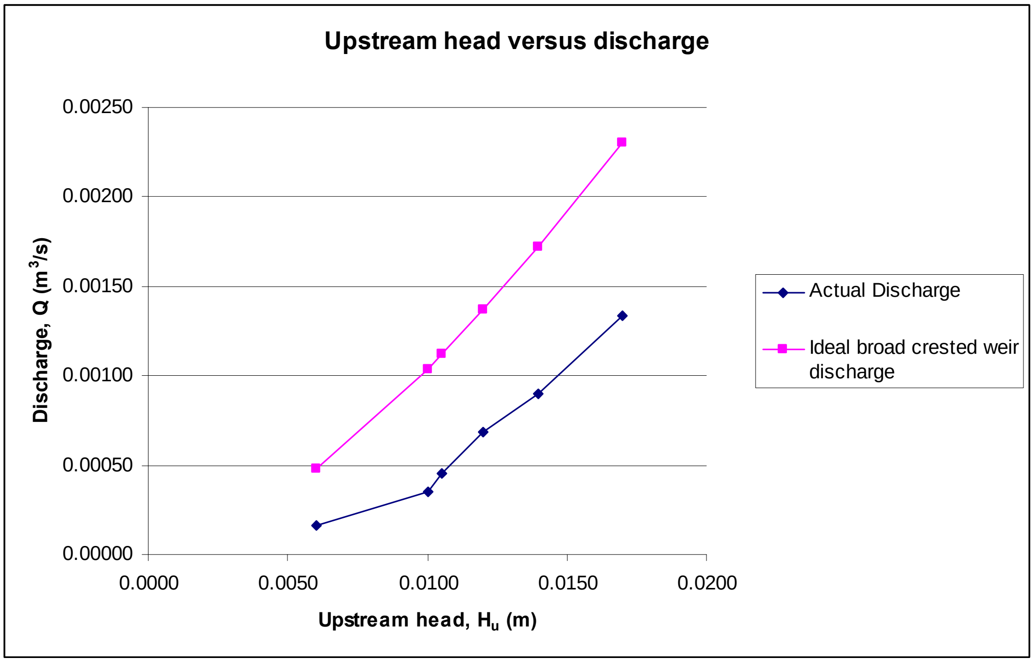

Figure 5.16 Transient flow. Actual discharge versus ideal broad crested weir flow

This graph shows that the head required for the measured discharges shown exceeds that of the ideal broad crested weir for the same discharge.

If equation 5.13 is applied to the measured data the following values for coefficient of discharge are calculated.

Table 5.25 Transient flow. Calculated coefficients of discharge

Q (m^3/s)	H_u (m)	C_d
0.00017	0.0060	0.3448
0.00035	0.0100	0.3365
0.00045	0.0105	0.4021
0.00068	0.0120	0.4998
0.00090	0.0140	0.5224
0.00133	0.0170	0.5784

The coefficients of discharge calculated are much smaller and vary much more than was expected. This indicates that the porous media has a huge influence on the flow in this phase.

Due to the resistance imposed by the porous media on the fluid, the transient phase of flow is not to be represented by the weir equation.

5.3.4 Transient flow

The method that best represents the transient range of flows is the gradually varied flow equation. This method accounts for the frictional resistance of the porous media and the depth of flow upstream and downstream of the weir.

5.4 Overflow

The overflow phase is reached once there is a measurable depth of flow over the downstream face of the weir. This phase is to be investigated by analogy to the general weir equation.

5.4.1 Overflow flow measurements

The measurements taken that represent the overflow phase of flow associated with the weir are as shown in table 5.26.

Table 5.26 Overflow flow. Measured values

Q (L/min)	d_u (mm)	d_{df} (mm)	d_o (mm)
185	98	7	0
201	99	7.5	1
234	102	8	2
259	103	8	3

Similar adjustments are made to the overflow measurements as were made to the submerged flow measurements in section 5.2.1. The final measurement shown here is the depth over the downstream face of the weir (d_o) and represents the depth of the overflow at this point. The location of this measurement is shown in figure 4.6.

Table 5.27 shows the corrected values to be used in the calculations.

Table 5.27 Overflow flow. Adjusted measurements

Q (L/min)	d_u (mm)	L_T (mm)	d_d (mm)	d_{df} (mm)	d_o (mm)
185	96	160	78	7	0
201	97	160	78	7.5	1
234	100	160	78	8	2
259	100.5	160	78	8	3

Table 5.28 shows the head upstream and the corresponding discharge.

Table 5.28 Overflow flow. Upstream head

Q (m^3/s)	H_u (m)
0.0031	0.0960
0.0034	0.0970
0.0039	0.1000
0.0043	0.1005

The discharge can then be plotted against the head upstream.

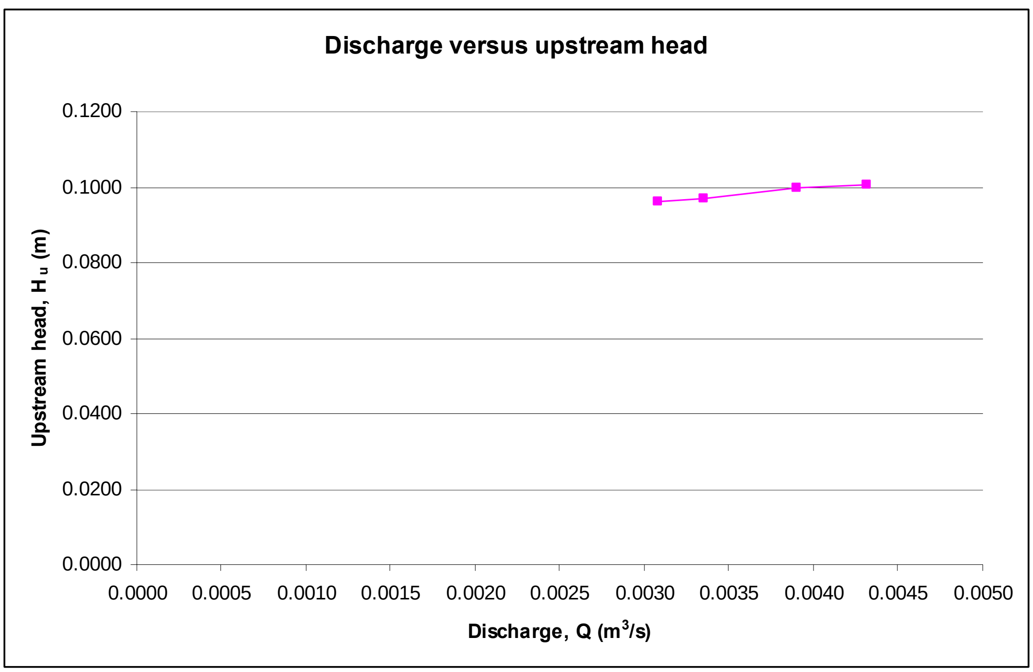

Figure 5.17 Overflow flow. Discharge versus upstream head

This plot (figure 5.17) shows that there is a very small increase in upstream head for a substantial increase in the discharge in comparison the submerged and transient flow regimes. This was expected, as when the flow is completely over the weir the porous media does not affect this portion of the discharge.

It is anticipated that the overflow component of the flow over the weir will be represented by the general weir equation. This general equation is as shown below.

$$Q = C \times H^{n}$$

If the flows were to become so large it is expected that the flow through the weir would be so minor that the flow profile would resemble that of an ideal broad crest weir. The equation representing the ideal flow over the broad crested weir from Chadwick and Morfett is,

$$Q_{ideal} = 1.705 \times w \times H^{3/2},$$

…Equation 5.14

where;

w =the width of the weir (m), and;
H = the head of water above the weir (m).

The following figure, 5.18, shows the relationship for the upstream depth and corresponding discharge an ideal broad crested weir. The basis for the weir is that the height of the sill is 0.078m, the same as that for the porous weir modelled. The ideal broad crested weir is impermeable and there will be no discharge until the depth over tops the crest height (as shown in figure 5.18 by the depth upstream of the weir equal to 0.078m and a corresponding discharge of zero).

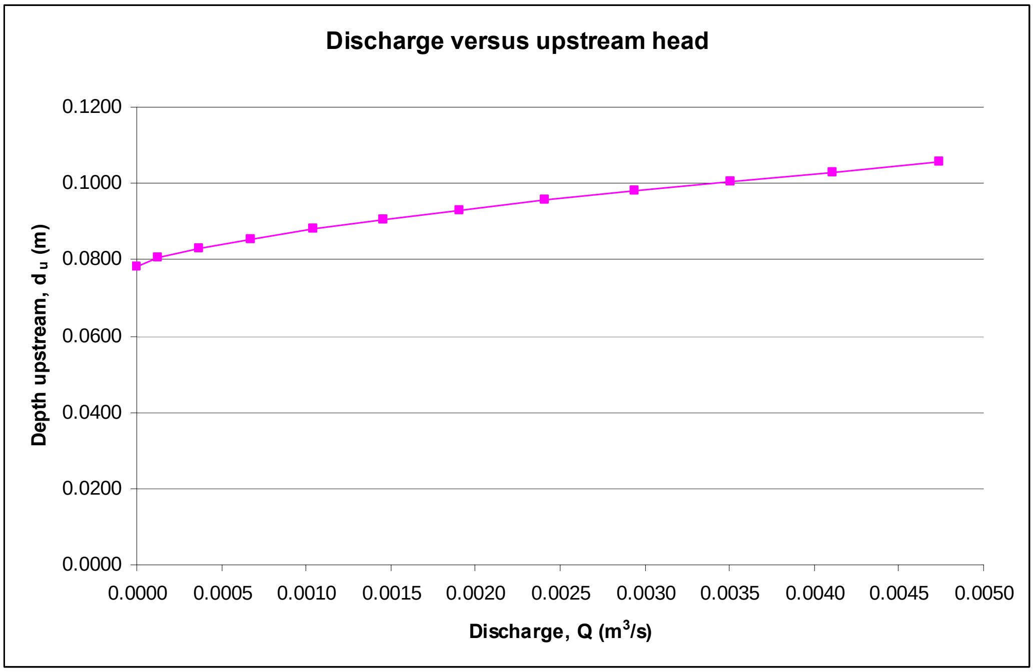

Figure 5.18 Overflow flow. Performance of the ideal broad crested hard weir

If the flow profile of the porous weir is overlaid, as in the figure 5.19, it can be seen that the profile of the flow over the weir closely resembles that of the hard weir when it is overflow is achieved.

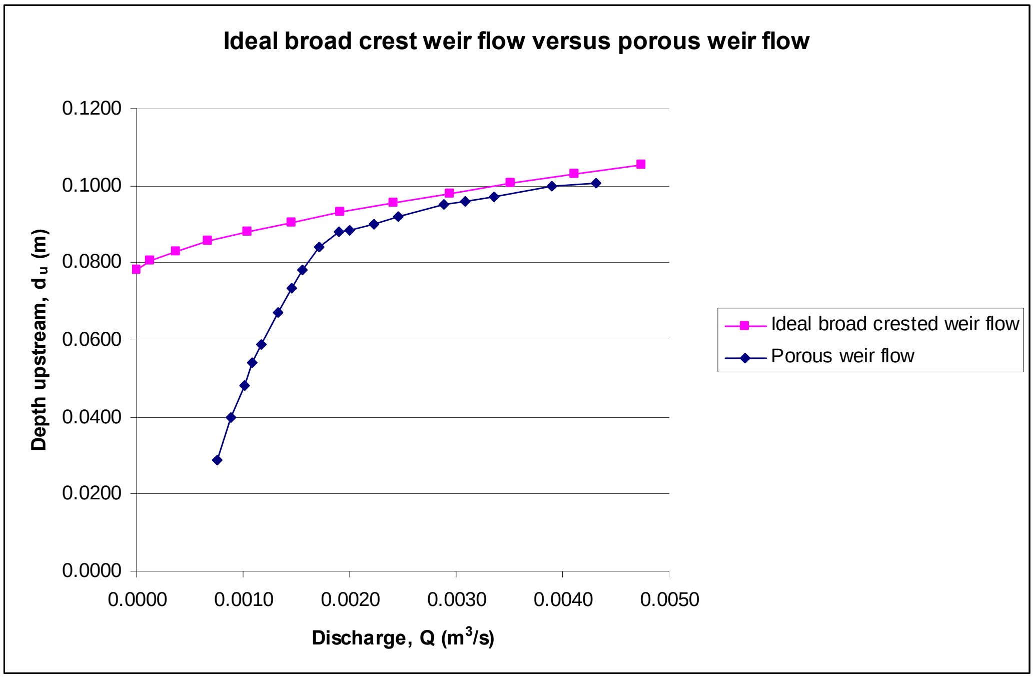

Figure 5.19 Overflow flow. Comparison between the modelled porous weir and the ideal broad crested hard weir

The difference in the discharge, for the ideal broad crested weir flow and the porous weir flow, for similar upstream depths can be accounted for by the additional flow through the porous weir when the same upstream depth is attained.

The trend at the higher discharges, in figure 5.19, shows the two profiles merging and the similarities between the two when overflow occurs. The apparent merging of the two profiles indicates that as the discharge increases indicates that the flow through the weir is less significant at the greater discharges where the majority of the flow is over the top of the weir.

In order to evaluate the performance of an identically sized impermeable weir, the porous weir model was wrapped in a thin plastic film and subject to a range of flows in the wide flume. If we add to the above graph the measurements obtain from testing the weir when in an impermeable state, the following figure 5.20 is attained.

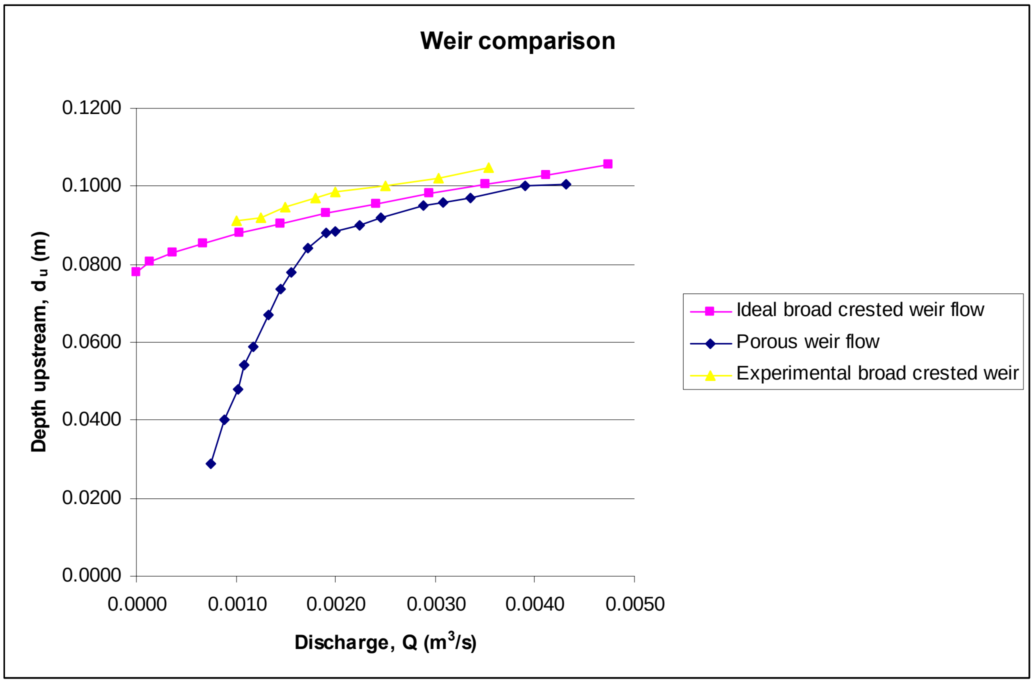

Figure 5.20 Overflow flow. Comparison between the modelled porous weir, the ideal broad crested hard weir and the modelled broad crested hard weir

Here it can be seen that the performance of the ideal broad crested weir requires less upstream head to achieve the same rate of discharge than the model of the broad crested weir. This is due to losses incurred as the flow passes over the weir. These losses are neglected in the ideal broad crested weir calculations.

The following plot shows the relationship observed if the submerged flow of $0.00155 m^3/s$ is added to the experimental broad crested weir and the ideal broad crested weir to calibrate the comparison to flow over the upstream face of the weir.

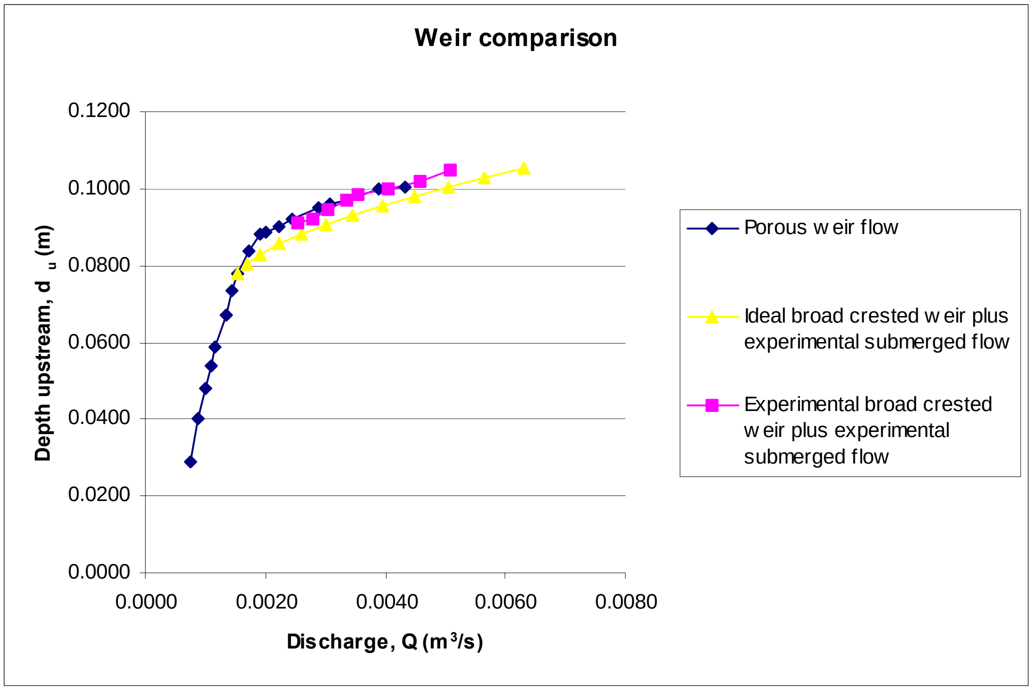

Figure 5.21 Overflow flow. Comparison between the modelled porous weir, the ideal broad crested hard weir with experimental submerged flows added and the modelled broad crested hard weir with experimental submerged flows added.

Figure 5.21 shows that the ideal broad crested weir would over estimated the discharge for a given upstream depth. The experimentally tested broad crested weir, however, shows a very good correlation between the measured upstream depth and discharge when compared to the actual measured flow through the porous weir.

There is a small discrepancy between the values of discharge in the transient phase. This is not of concern as the method of determining the transient flow by the gradual varied flow equation as outlined in section 5.4.

Application of equation 5.13 to the measured data from the experimental broad crested weir will allow the determination of the coefficient of discharge (C_d). Table 5.29 shows the values of the coefficient of discharge calculated.

Table 5.29 Overflow flow. Upstream head versus coefficient of discharge

Q (m^3/s)	H_u (m)	C_d
0.0010	0.0130	0.6487
0.0013	0.0140	0.7255
0.0015	0.0165	0.6805
0.0018	0.0190	0.6608
0.0020	0.0205	0.6552
0.0025	0.0220	0.7366
0.0030	0.0240	0.7844
0.0035	0.0270	0.7657

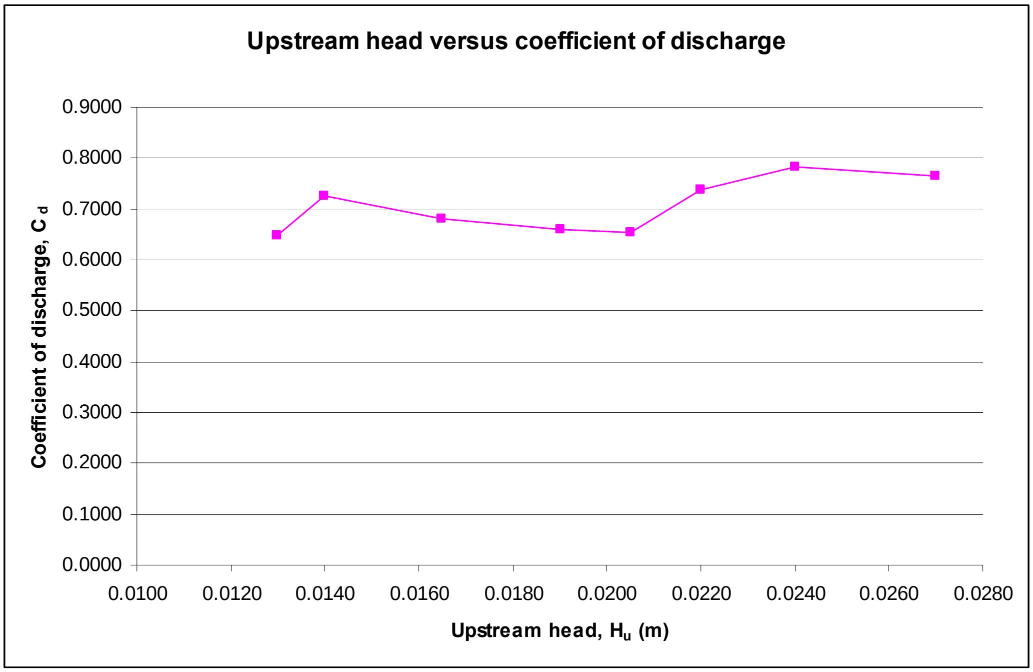

Figure 5.22 Overflow flow. Upstream head versus coefficient of discharge

The coefficient of discharge is not usually a constant value, but generally increases as the depth of flow over the top of the weir increases. In this case it is assumed that the coefficient of discharge is constant as the depth of flow over the weir is very small over the entire range of flows measured. If we take the average of the coefficient of discharge calculated in table 5.29, a coefficient of discharge equal to 0.7072 is obtained.

By adopting the coefficient of discharge equal to 0.7072 and using equation 5.13, the discharge in the overflow phase can be determined.

5.5 The complete range of flows

Figure 5.23 represents the entire range of flows and shows the discharge versus upstream head relationship for the flow upstream of the weir.

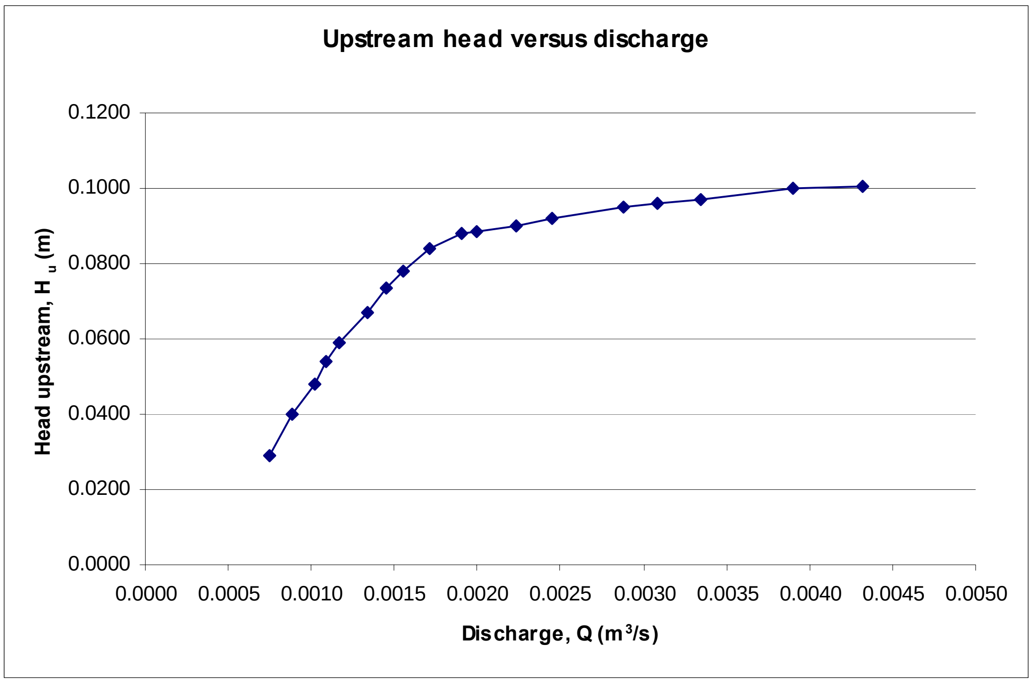

Figure 5.23 Total flow. Discharge versus upstream head

It was shown in the submerged range, the flow could be represented by the equation,

$$f = \frac{L}{A_u}\left(S_0 - \frac{dy}{dx}\left(1 - \alpha\frac{Q^2 w}{A_u^3 g}\right)\right),$$

where the friction factor (f) is equal to 1.418.

Once the upstream depth exceeds the height of the upstream face the flow moves into the transient zone, the flow can still be represented by the gradually varied flow equation where the friction factor is still equal to 1.418. This equation is still considered appropriate for this phase as the entire flow passes through the porous media. The friction factor accounts for the interaction between the porous media and the discharging fluid.

The overflow is defined by the broad crested weir equation where the coefficient of discharge is equal to 0.7072. The head used in the equation is based on the depth of flow over the top of the upstream face of the weir.

When these three phases are combined the following correlation, between the measured data and the theoretical data, is obtained and shown in figure 5.24.

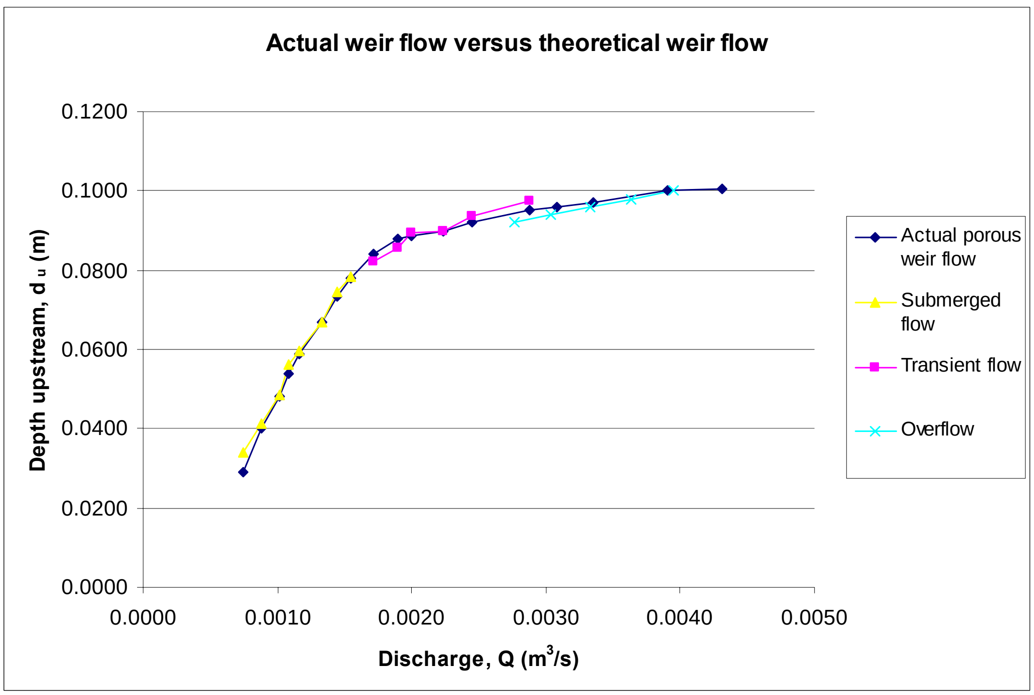

Figure 5.24 Total flow. Experimental versus theoretical discharges

It is observed that the weir equation for overflow overlaps with the transient flow and the calculated figures do not correlate well. This is because the depth of flow used in the weir equation is the depth over the upstream face of the weir (the start of the transient phase). The governing equation in the transient phase is the general equation for gradually varied flow. It is anticipated that at the upper limit of the transient phase the weir equation and the gradually varied flow equation will coincide. The gradually varied flow equation will then be disregarded and the broad crested weir equation for the overflow will represent the discharge.

RECOMMENDATIONS FOR FURTHER STUDY

For this type of structure to be adopted as a flood mitigation structure much more work needs to be done to establish better performance relationships between the porous media and the discharge characteristics.

This study has shown that for the weir size and the porous media characteristics, that the discharge can be related to a gradually varied flow equation where the flow is through the porous weir only. Once the weir is overtopped by the discharge, the overflow can be represented by a broad crested weir equation.

Further investigation into different combinations of weir size and porous media type will be required to verify that the correlations presented in this report stand up to the influence of the different weir properties.

Once this work has been done, investigation could turn the focus of the study to how the fluid moves through the weir, so the fluids behaviour can be understood in relation to the interaction between the porous media and the fluid.

Areas that could be included in further study include investigation into the velocity profiles through the weir, for example is the velocity greater along the base of the weir where the upstream pressure is greater at this depth.

Analysis of the flow in two dimensions could play an important role in determining the performance of the weir. A difference was observed between the depth of the storage upstream of the weir and the depth of the discharge from the downstream face of the weir.

CONCLUSION

The literature review was undertaken and no specific design parameters, standards or publish data was revealed. However important equations relating to porous media flow were discovered. The important porous media properties were revealed to be the diameter of the particles, the shape and porosity. Another key of the porous media to be the porosity and has been used extensively in porous media flow analysis.

The porous weir was successfully constructed and tested in the wide flume in the USQ hydraulics laboratory. The weir was subjected to flows ranging from 45L/min to 259L/min.

Three phases of flow were identified to occur during the complete range of flows experienced by the model of the porous weir tested in the wide flume. These flows were submerged, transient and overflow.

In the submerged phase of flow, calculations were undertaken to determine the type of flow through the weir. The flow was convincingly showed to be turbulent. Consequently the traditional Darcy equation did not yield a relationship to the flow experienced through the weir. It was also shown that some of the other Darcy based equations did not provide the reported correlation for the flow through the porous weir.

However a relationship was formed between the upstream head and the discharge for the entire range of flows experienced by the porous weir.

The submerged flow through the weir returned an excellent relationship to the general equation of gradually varied flow and a constant value for the associated friction factor of 1.418. This value is representative of the porous media used in the porous weir.

The transient flow was also related to the general equation of gradually varied flow and the friction factor of 1.418. This relationship worked well in this phase as the entire flow is still through the weir and is influenced by the porous media.

The overflow phase was represented by the broad crested weir equation. This is because the when flow overtops the weir the overflow component resembles traditional hard weir flow. The broad crested weir equation showed a good correlation to the measured porous weir data when the coefficient of discharge was equal to 0.7072.

REFERENCES

AS2758.4-2000, Aggregate for gabion baskets and wire mattresses 2000, Australian Standard, viewed 26 April 2006, < http://www.saiglobal.com/online/autologin.asp >

Bear J 1988, Dynamics of Fluids in Porous Media, Dover Publications INC, New York

Chadwick A & Morfett J 2002, Hydraulics in Civil and Environmental Engineering, Spon Press, London and New York

Das Braja M 1985, Advanced soil mechanics, McGraw Hill Book Company. Singapore

Fair, EJ 2004, CIV2402 Soil Mechanics: study book, University of Southern Queensland, Toowoomba

Kirkham, C E February 1967, Turbulent flow in porous media, University of Melbourne

Main Roads 2002, Road Drainage Design Manual, viewed 24 April 2006, <http://www.mainroads.qld.gov.au/MRWEB/Prod/Content.nsf/fbadb90201547b374a2569e700071c81/dc2b2ef83f579a754a256c31007fd506/$FILE/5a_chapter%205%20no%20Appendices.pdf>

Michioku K, Maeno S, Furusawa T & Haneda M 2005, 'Discharge through a Permeable Rubble Mound Weir', Journal of Hydraulic Engineering, viewed 09 April 2006, <http://scitation.aip.org/getpdf/servlet/GetPDFServlet?filetype=pdf&id=JHEND80001310000001000001000001&idtype=cvips&prog=normal>

Nalluri C & Featherstone R E 2001, Civil Engineering Hydraulics, Alden Press Ltd, Oxford and Northampton

Singh, A 1967, Soil Engineering in Theory and Practice, Asia Publishing House, Bombay

Venkataraman P & Rama Mohan Rao P 1998, ‘Darcian, Transitional, and Turbulent Flow through Porous Media’, Journal of Hydraulic Engineering, viewed 09 April 2006, <http://scitation.aip.org/getabs/servlet/GetabsServlet?prog=normal&id=JHEND800012400000800084000001&idtype=cvips&gifs=yes>

BIBLIOGRAPHY

Cedergren H 1989, Seepage, Drainage, and flow nets, John Wiley & Sons, Inc

Ettena R (chair and editor) 2000, Hydraulic Modeling: Concepts and Practice, American Society of Civil Engineers

Van Gent M R A 1995, 'Porous Flow Through a Permeable Rubble Mound Weir', Journal of Waterway, Port, Coastal, and Ocean Engineering, veiwed 09 April 2006, <http://scitation.aip.org/getpdf/servlet/GetPDFServlet?filetype=pdf&id=JHEND8000 131000001000001000001&idtype=cvips&prog=normal>

APPENDIX A.1 Program specification, Issue B

University of Southern Queensland

Faculty of Engineering and Surveying

ENG4111/4112 Research Project

Project Specification

For : Joseph Saunders

Topic : Porous Weirs for Flood Mitigation

Supervisor : Ken Moore

Project Aim : To evaluate the performance of a porous weir by analysing different stages of flow and to develop head discharge relationship for the porous weir.

Program: Issue B, 12 October 2006

1. Conduct a literature review to determine design parameters and standards, and hydraulic performance of various flood mitigation structures for urban stormwater drainage with particular emphasis on weirs. Include investigation of any published data concerning the head discharge characteristics of porous weirs.

2. Design and construct a scale model of a porous weir, taking into account researched weir design parameters.

3. Measure the hydraulic performance by testing the model in the USQ Hydraulics Laboratory under a range of head and tailwater conditions. If time and/or resources allow, test the model using different sized media and weir dimensions.

4. Develop a relationship between the head and the discharge using known parameters of the porous media.

5. If time permits, scale the model to full scale and compare the performance of the porous weir to a traditional hard weir.

6. If time permits, conduct an economical analysis to compare the costs of porous weirs to that of 'hard' weirs of similar head discharge characteristics.

7. Prepare recommendations on the use of porous weirs for flood mitigation purposes.

AGREED J Saunders student   K Moore supervisor

12/10/06 date

APPENDIX A.2 Program specification, Issue A

Faculty of Engineering and Surveying

ENG4111/4112 Research Project

Project Specification

For	:	Joseph Saunders
Topic	:	Porous Weirs for Flood Mitigation
Supervisor	:	Ken Moore
Project Aim	:	To develop head-discharge relationships for porous weirs of various configurations and to use these data to compare the flood mitigation effect of full scale porous weirs with that of conventional 'hard' weirs using an appropriate hydrologic model.

Program: Issue A, 27 March 2006

1. Conduct a literature review to determine design parameters and standards, cost effectiveness and hydraulic performance of various flood mitigation structures for urban stormwater drainage with particular emphasis on weirs. Include investigation of any published data concerning the head-discharge characteristics of porous weirs.
2. Design and construct scale models of porous weirs incorporating various cross section geometries and particle size graduations.
3. Determine the hydraulic characteristics by testing the scale models in the flume of the USQ Hydraulics Laboratory under various head and tailwater conditions. If time and/or resources allow, investigate the potential and subsequent hydraulic effect of partial blockage of the weir due to floating and/or suspended debris.
4. Using the test data, develop full scale hydraulic characteristics of porous weirs using appropriate scaling techniques.
5. Using a suitable hydrologic computer model applied to a real or hypothetical catchment, compare the flood mitigation effect of porous weirs with that of conventional 'hard' structures based on design and/or recorded rainfall events.
6. If time permits, conduct an economic analysis to compare costs of porous weirs against that of 'hard' weirs of similar head-discharge characteristic.
7. Prepare recommendations on the use of porous weirs for flood mitigation purposes.

AGREED ____________, student KQ Moore ____________ supervisor

27/3/2006 date

APPENDIX B Construction drawings

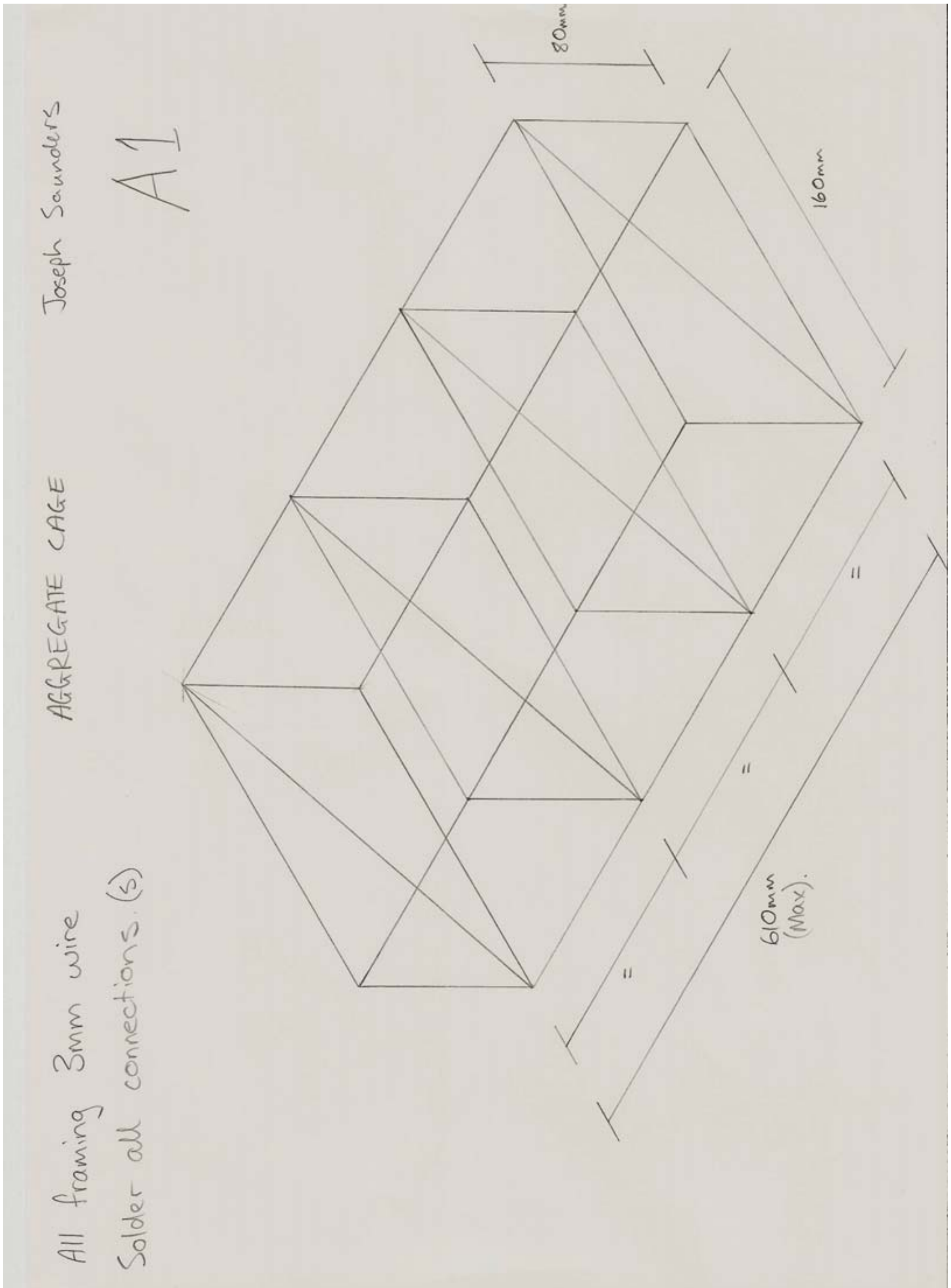

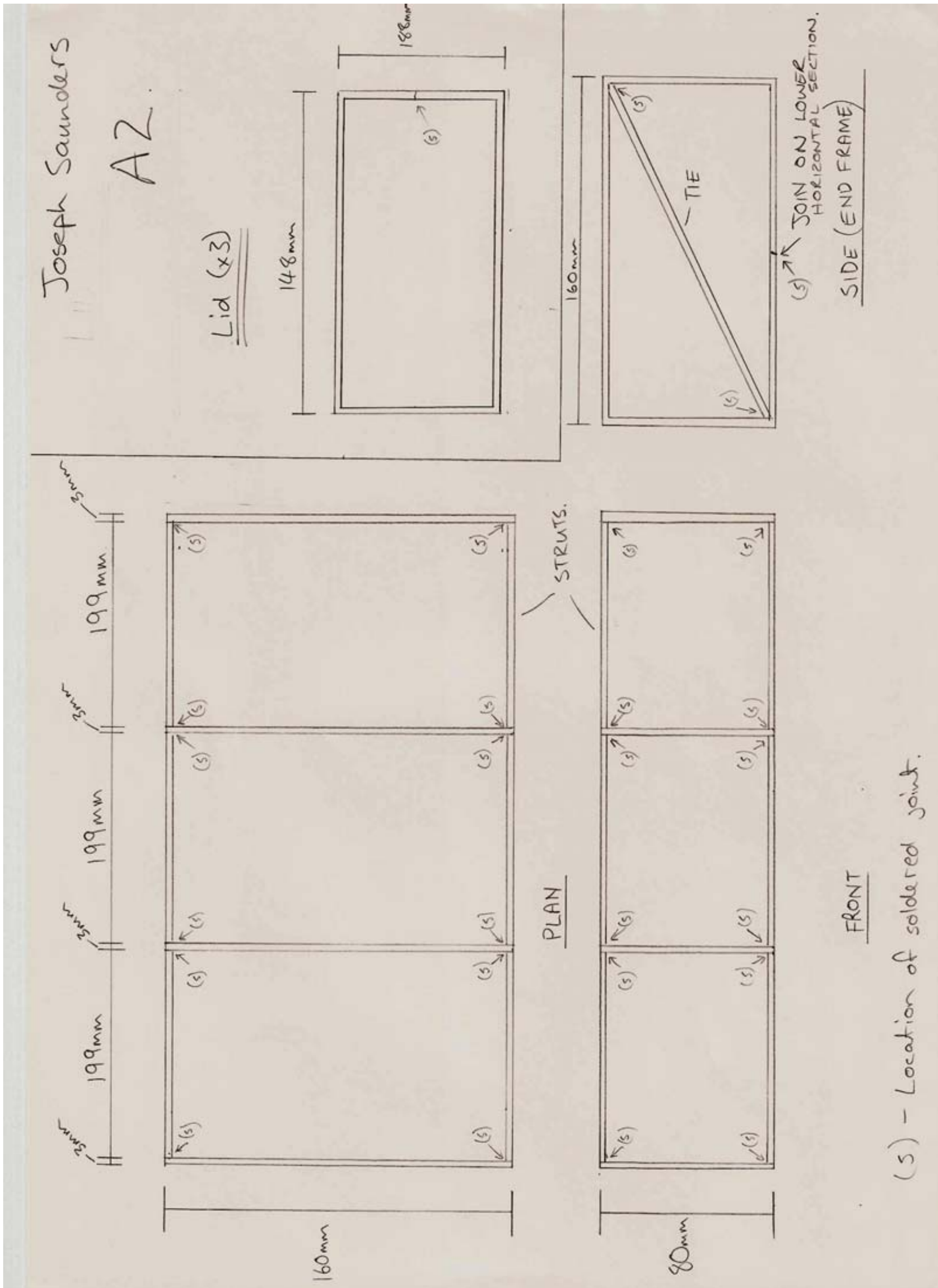
Joseph Saunders
A2.
Lid (x3)
148mm
188mm
160mm
TIE
(S) JOIN ON LOWER HORIZONTAL SECTION.
SIDE (END FRAME)
3mm
199mm
3mm
199mm
3mm
199mm
3mm
STRUTS.
PLAN
FRONT
160mm
80mm
(S) - Location of soldered joint.